IVYSPRING INTERNATIONAL PUBLISHER

Theranostics

2020; 10(6): 2597-2611. doi: 10.7150/thno.40595

Research Paper

Coronary artery mechanics induces human saphenous vein remodelling *via* recruitment of adventitial myofibroblast-like cells mediated by Thrombospondin-1

Gloria Garoffolo[1,2*], Matthijs S. Ruiter[1*], Marco Piola[3] , Maura Brioschi[4], Anita C. Thomas[5], Marco Agrifoglio[6], Gianluca Polvani[6], Lorenzo Coppadoro[3], Stefano Zoli[7], Claudio Saccu[7], Gaia Spinetti[8], Cristina Banfi[4], Gianfranco B. Fiore[3], Paolo Madeddu[5], Monica Soncini[3] and Maurizio Pesce[1]✉

1. Unità di Ingegneria Tissutale Cardiovascolare; Centro Cardiologico Monzino, IRCCS; Milan, Italy
2. PhD Program in Translational and Molecular Medicine – DIMET; Università di Milano - Bicocca, Milan, Italy
3. Dipartimento di Elettronica, Informazione e Bioingegneria; Politecnico di Milano; Milan, Italy
4. Unità di Proteomica; Centro Cardiologico Monzino, IRCCS, Milan, Italy
5. Bristol Heart Institute, University of Bristol; Bristol, UK
6. Dipartimento di Scienze Cliniche e di Comunità; Università di Milano, Milan, Italy; Centro Cardiologico Monzino, IRCCS, Milan, Italy
7. Unità di Chirurgia Vascolare, Centro Cardiologico Monzino, IRCCS; Milan, Italy
8. IRCCS Multimedica, Milan, Italy

*Equal contribution

✉ Corresponding author: Maurizio Pesce, PhD, Unità di Ingegneria Tissutale Cardiovascolare; Centro Cardiologico Monzino, IRCCS; Via C. Parea, 4; 20138, Milan, Italy.

Received: 2019.09.24; Accepted: 2019.11.22; Published: 2020.02.03

Abstract

Rationale: Despite the preferred application of arterial conduits, the greater saphenous vein (SV) remains indispensable for coronary bypass grafting (CABG), especially in multi-vessel coronary artery disease (CAD). The objective of the present work was to address the role of mechanical forces in the activation of maladaptive vein bypass remodeling, a process determining progressive occlusion and recurrence of ischemic heart disease.

Methods: We employed a custom bioreactor to mimic the coronary shear and wall mechanics in human SV vascular conduits and reproduce experimentally the biomechanical conditions of coronary grafting and analyzed vein remodeling process by histology, histochemistry and immunofluorescence. We also subjected vein-derived cells to cyclic uniaxial mechanical stimulation in culture, followed by phenotypic and molecular characterization using RNA and proteomic methods. We finally validated our results *in vitro* and using a model of SV carotid interposition in pigs.

Results: Exposure to pulsatile flow determined a remodeling process of the vascular wall involving reduction in media thickness. Smooth muscle cells (SMCs) underwent conversion from contractile to synthetic phenotype. A time-dependent increase in proliferating cells expressing mesenchymal (CD44) and early SMC (SM22α) markers, apparently recruited from the SV adventitia, was observed especially in CABG-stimulated vessels. Mechanically stimulated SMCs underwent transition from contractile to synthetic phenotype. MALDI-TOF-based secretome analysis revealed a consistent release of Thrombospondin-1 (TSP-1), a matricellular protein involved in TGF-β-dependent signaling. TSP-1 had a direct chemotactic effect on SV adventitia resident progenitors (SVPs); this effects was inhibited by blocking TSP-1 receptor CD47. The involvement of TSP-1 in adventitial progenitor cells differentiation and graft intima hyperplasia was finally contextualized in the TGF-β-dependent pathway, and validated in a saphenous vein into carotid interposition pig model.

Conclusions: Our results provide the evidence of a matricellular mechanism involved in the human vein arterialization process controlled by alterations in tissue mechanics, and open the way to novel potential strategies to block VGD progression based on targeting cell mechanosensing-related effectors.

Key words: coronary artery bypass grafting, vein graft disease, mechanotransduction, Thrombospondin-1, arterialization

Introduction

Coronary artery bypass grafting is used in cardiac surgery for more than 50 years to combat the consequences of coronary artery disease [1-3], a pathology with a wide incidence in Western world (> 1000 cases/ 10^6 adult people) and rapidly increasing in emerging countries – e.g. China [4]. The most represented coronary-compatible vessels used in CABG are the internal mammary artery (IMA), the radial artery (RA) and the SV. The patency of arterial grafts is relatively well preserved, while the SV conduits are subject to intima hyperplasia determining progressive graft occlusion. In a high percentage of cases, this requires re-hospitalization with graft stenting and, ultimately, re-intervention [1, 2]. More in details, early vein graft failure due to acute thrombosis occurs in as many as 18% of cases. Intermediate graft failure (up to 2 years after surgery), and late graft failure (> 2 years after surgery), occurs in 20% to 50% of cases at 5 years. Finally, by 10 years after surgery, 40% of grafts result completely blocked and a further 30% have a compromised flow. Even if early remodelling of the vein is predictive for later graft patency, the aetiology of long-term failure is still poorly understood [5]. Initially, both the surgical procedure and exposure to high flow and pressure compromise the endothelial layer, which induce SMCs proliferation [6, 7], changes in matrix composition, and thickening/stiffening of the vessel wall. This limits the vein's adaptability to the arterial circulation and ultimately leads to clinically apparent stenosis [8]. Animal models revealed that occlusion of autologous SV grafts is a consequence of neointima formation, driven by proliferation and migration of SMCs and possibly of adventitial progenitors into the intima [9], inducing extracellular matrix (ECM) deposition, and formation of a thick neointima [10].

The role of mechanical forces in the progression of graft failure has been recognized, although the nature of cell-based mechanosensing in the vascular tissue remains unclear due the difficulty of decoupling distinct components *in vivo* [11, 12]. In fact, the existing studies have not yielded conclusive results on the effect of mechanical stimulation on SMC growth and phenotype, with results depending on direction, frequency, duration and modality of the stimulus, but also on the origin and initial phenotype of the SMCs. For example, cyclic strain of human SV-derived SMCs resulted in increased DNA synthesis and cell number with a decrease in smooth muscle α-actin (αSMA) [13-15], while cells of arterial origin showed opposite effects [16, 17]. *Ex vivo* vessel culture systems (EVCSs) and bioreactors to stimulate cells mechanically offer the unique possibility to investigate the effects of isolated or combined mechanical stimuli under well-controlled and reproducible biomechanical and/or metabolic conditions in human large vessels. In this framework, the aim of the present investigation was to characterize the effect of coronary mechanical conditions on molecular programming of vein graft disease using an integrated tissue/cell biomechanical approach.

Methods

Extended Methods are provided in the Methods section in the online only Data Supplement.

Ethics

The experimental investigation on human-derived tissues and cells was approved by the local ethical Committee at Centro Cardiologico Monzino, IRCCS. Patients were required to sign an informed consent. The use of human material was done in compliance with the Declaration of Helsinki. The main patient characteristics are shown in Table S1. Arteriovenous bypass procedures in pigs were performed in female Landrace or Large White/ Landrace crossbred pigs weighing 20 to 30 kg. All animals received humane care in accordance with the Home Office Animals (Scientific Procedures) Act of 1986 and the Guide for the Care and Use of Laboratory Animals published by the US National Institutes of Health (NIH Publication No. 85- 23, revised 1996). For surgery, anaesthesia was induced with a single dose of intramuscular ketamine into the neck (0.1 mg/Kg ketamine: Ketaset Injection Fort Dodge Animal Health Ltd, Southampton, UK). After endotracheal intubation, anaesthesia was maintained using 2-3% halothane and oxygen, the animals ventilating spontaneously throughout. Animals were euthanized with 100 mg/Kg intracardiac injection of pentobarbitone in a single dose (Euthatal; 200 mg/mL pentobarbital sodium, J.M. Loveridge Plc, Southampton, UK).

Tissue/cells mechanical stimulations

Mechanical stimulations of SV grafts were performed using a custom-made bioreactor [18] tailored to reproduce the coronary mechanics. Cell straining was performed with Flex-Cell system. Mechanical stimulation times ranged from 7 to 14 days for SV grafts and from 1 to 3 days for cells.

Tissue/cells analyses

After mechanical stimulation, tissues, cells and culture supernatants were prepared and appropriately processed for histological, immunohistochemical, immunofluorescence, protein/secretome and RNA analyses, as already published [19], and described in the extended online methods.

In vitro cell culture

Isolation of cells for *in vitro* experiments was performed as previously described [20, 21], using immunomagnetic and/or plastic adherence selection. Migration experiments were performed using Transwell-based assays followed by quantification of Crystal-Violet cell staining.

Molecular analyses

Tissue/cells RNA and protein content was analysed by Q-RT-PCR and Western blotting performed with protocols already published [19], while the secretome analysis was conducted using a MALDI-TOF methods as already described [22].

Data representation and statistical analyses

In all graphs throughout the manuscript, data were plotted as mean ± standard error using GraphPad Prism 7. A P value < 0.05 was considered significant. The type of statistical test employed for data comparison is specified in figure legends. As a general rule, comparisons between two independent samples were performed by unpaired/paired t-test (two-tails), while for comparisons between 3 or more groups we adopted one-way ANOVA with post-hoc comparisons tests. The specification of the number of independent samples included in the analyses and the type of statistical tests used to compare data are specified in the legends to figures. Further details about data processing are provided in the online methods section.

Results

CABG-like hemodynamics induces consistent remodeling of human SV wall associated to SMCs phenotypic switching

Our previous contributions showed that application of an 80-120 mmHg pulsatile pressure regimen determined a change in the SV structure at 7 days, consisting of a significant thinning of the vessel wall, and elevation in cell death by apoptosis and enhanced proliferation [18, 19]. These changes were less evident in SVs exposed to venous flow (VP), characterized by a constant low pressure (5 mmHg). Confirming these findings, morphometric analyses of SVs treated with coronary flow showed a significant thinning of the medial layer (Figure 1A-B). In order to demonstrate the specific effects of mechanical forces on intima thickening, we compared results obtained in the presence of venous or coronary flow/pressure patterns with a conventional vein 'rings' culturing model[23]. Figure S1 and S2 show results of this experiment, which demonstrate that in the presence of coronary flow-pressure pattern intima thickening does not occur, at least at the considered time points.

Since *ex vivo* cultured SVs exhibited a similarly elevated cellular apoptosis (Figure 2A-B), we investigated whether application of a coronary-like flow pattern affected the phenotype of the surviving cells. To this aim, we performed IF staining with antibodies recognizing SMCs contractile markers αSMA (Figure 3A)/Calponin (Figure 3B), and the synthetic SMCs marker Vimentin (Figure 3C). Cells quantification (Figure 3D) demonstrated a clear reduction in the percentage of αSMA^+ and $Calp^+$ cells in SV conduits stimulated with coronary flow/ pressure pattern, and a consistent increase in cells with synthetic characteristics, suggesting a SMCs phenotypic transition.

Coronary mechanics induces recruitment and proliferation of $CD44^+$ cells in SV medial layer

Recruitment of cells from the vascular adventitia has been identified as a key early event in VGD setting in animal vein arterialization models [24]. Furthermore, microscopic observations performed in explanted CABGs or SV grafts exposed *ex vivo* to *trans*-wall hypoxia gradients showed an enhanced growth of adventitia vessels [25]. Since CD44 marker expression has been associated to myofibroblast programming of stromal cells in fibrotic diseases [26, 27], we investigated the expression of this marker after culturing SV grafts. In order to assess if cells expressing CD44 also expressed SMCs markers, we performed co-staining with anti-αSMA and -SM22α specific antibodies in control and *ex vivo* cultured SVs. As shown in Figure 4A-B very few $CD44^+$ cells were present in the media of the vessels before the beginning of the culture. However, these cells increased time-dependently, in particular in CABG samples, where they exhibited a clear co-staining with SM22a. Quantification of cells confirmed that $CD44^+$ and $SM22\alpha^+$ cell percentages increased under either VP or CABG stimulation at day 7, and continued to rise in CABG-stimulated vessels at day 14 (Figure 4C). The presence of $CD44^+/SM22\alpha^+$ cells in CABG-treated SVs exhibited, finally, a substantial and constant increase (Figure 4C). Since the majority of $CD44^+$ and $SM22\alpha^+$ cells at the beginning of the culture were confined in the adventitia in close association with the *vasa vasorum* (Figure S3), this suggests that coronary flow/pressure pattern activates adventitial cells expressing myofibroblasts/immature SMCs markers. In keeping with this conclusion, increase in $CD44^+/SM22\alpha^+$ cells in CABG-stimulated grafts was associated to an elevated proliferation level (Figure 5A-C), which was more pronounced initially in the adventitia (in particular in the *vasa vasorum* region), and later in the media, as detected by expression of PCNA marker.

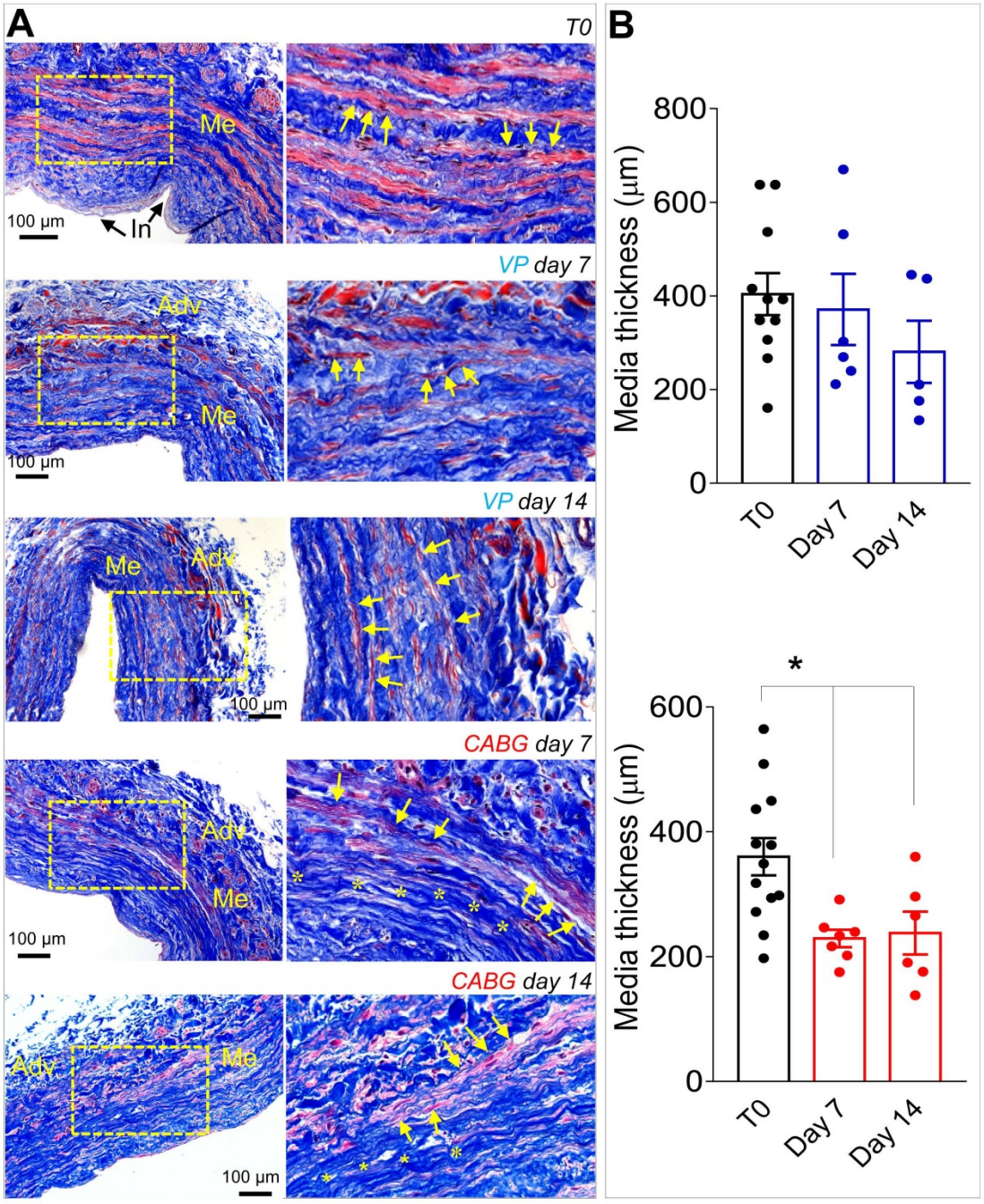

Figure 1. (A) Low and high magnifications (zones enclosed in the yellow areas) of transversal sections of native SVs (T0) and SVs exposed to venous perfusion (VP) or coronary flow (CABG) for 7 and 14 days, stained with Masson's trichrome. While in VP samples, the circumferentially arranged SMCs bundles (characterized by the red staining, yellow arrows) are present throughout the culturing period, in SVs exposed to CABG mechanics, part of these bundles disappeared (areas stained in blue, asterisks) leaving zones rich in collagen and deprived of cells. This suggests that circumferential SMCs bundles are a specific target of coronary flow mechanics. (B) Quantification of media thickness, confirmed a major effect of the CABG stimulation on SV wall remodeling. * indicate $P < 0.05$ by one-way ANOVA with Newman-Keuls post-hoc. Bar graphs represent mean and SE. Me = Media; Adv = Adventitia: In = Intima.

Thrombospondin-1 is a mechanically regulated factor in the SV wall associated to SMCs switching from contractile to synthetic phenotype

Mechanical forces exerted by the counter-pulsed coronary flow on vein wall expose vein-resident cells to a high level of strain, whose distribution is modified compared to the natural venous perfusion [12]. We then modelled *in silico* the level of cell deformation associated to the circumferential strain of the two major SV layers occurring in the presence of coronary flow mechanics. We were interested in this strain component considering the orientation of the circumferentially arranged SMCs bundles, which appeared the most affected structures in the media of CABG-stimulated SV conduits (Figures 1 and 3). As shown in Figure 6A, the model predicted a more

pronounced strain in the stiffer media (~ 26% elongation), and a lower strain value (~ 18% elongation) in the softer adventitia. Based on this evaluation, we decided to investigate the effects of uniaxial cell deformation on SMCs isolated from human SVs (Figure S4) using an *in vitro* cyclic cell strain setting. Figures S5 and 6B show the results of 24 and 72 h SMCs mechanical stimulation, which determined a significant reorientation of the cells. Under these conditions, these cells downregulated the contractile phenotype marker αSMA, and upregulated the levels of Vimentin (Figure 6B). They also exhibited a substantial rearrangement of the contractile cytoskeleton organization, which acquired an arrangement consistent with the synthetic phenotype [21] (Figure S6).

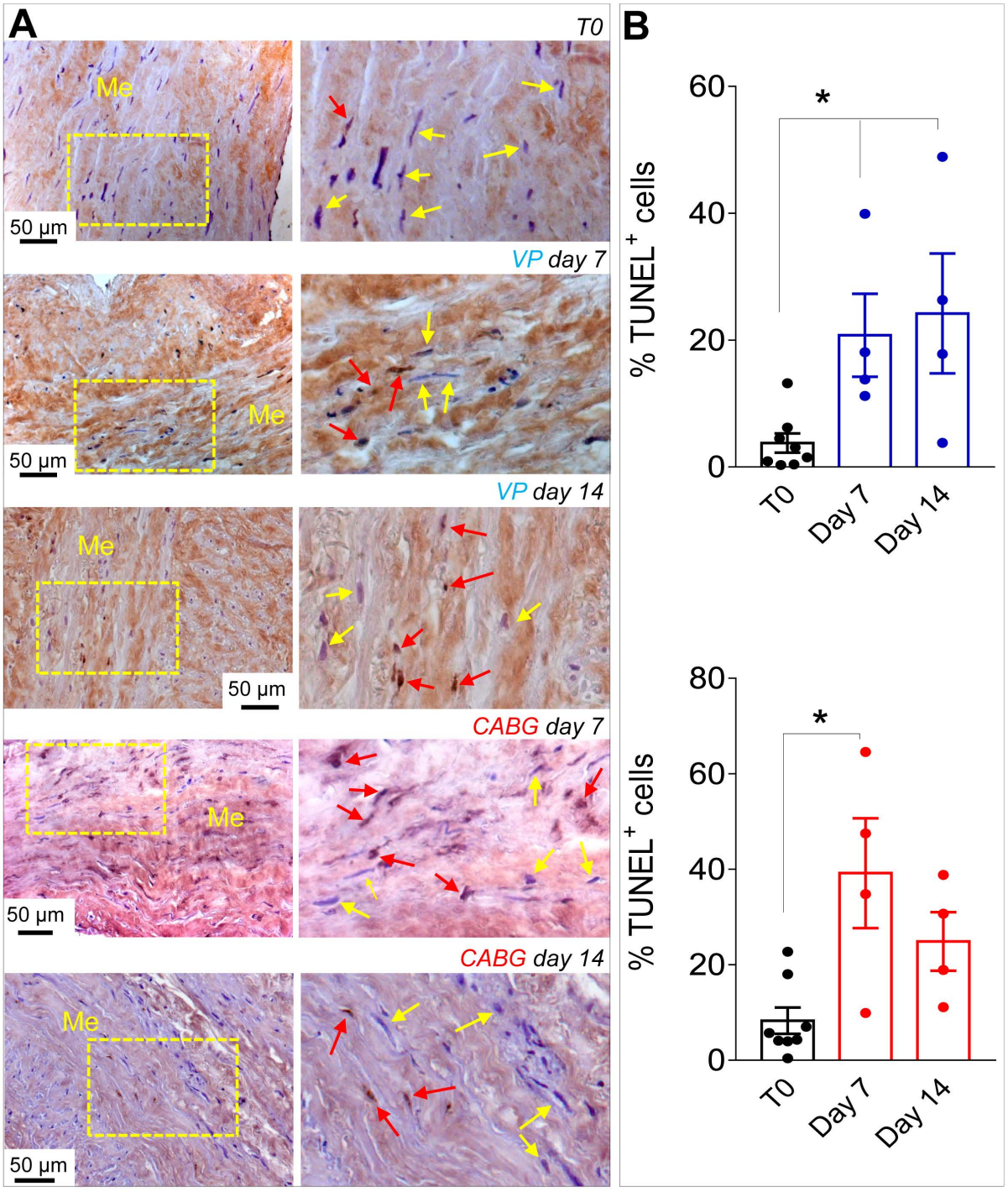

Figure 2. (A) Low and high magnifications (zones enclosed in the yellow areas) of transversal sections of native SVs (T0) and SVs exposed to venous perfusion (VP) or coronary flow (CABG) for 7 and 14 days stained with TUNEL assay for detection of apoptotic cells. Yellow arrows indicate TUNEL⁻ cells while red arrows indicate TUNEL⁺ apoptotic cells. (B) Apoptosis quantification in the SV media at the two time points. * indicate $P < 0.05$ by one-way ANOVA with Newman-Keuls post-hoc. Bar graphs represent mean and SE. Me = Media.

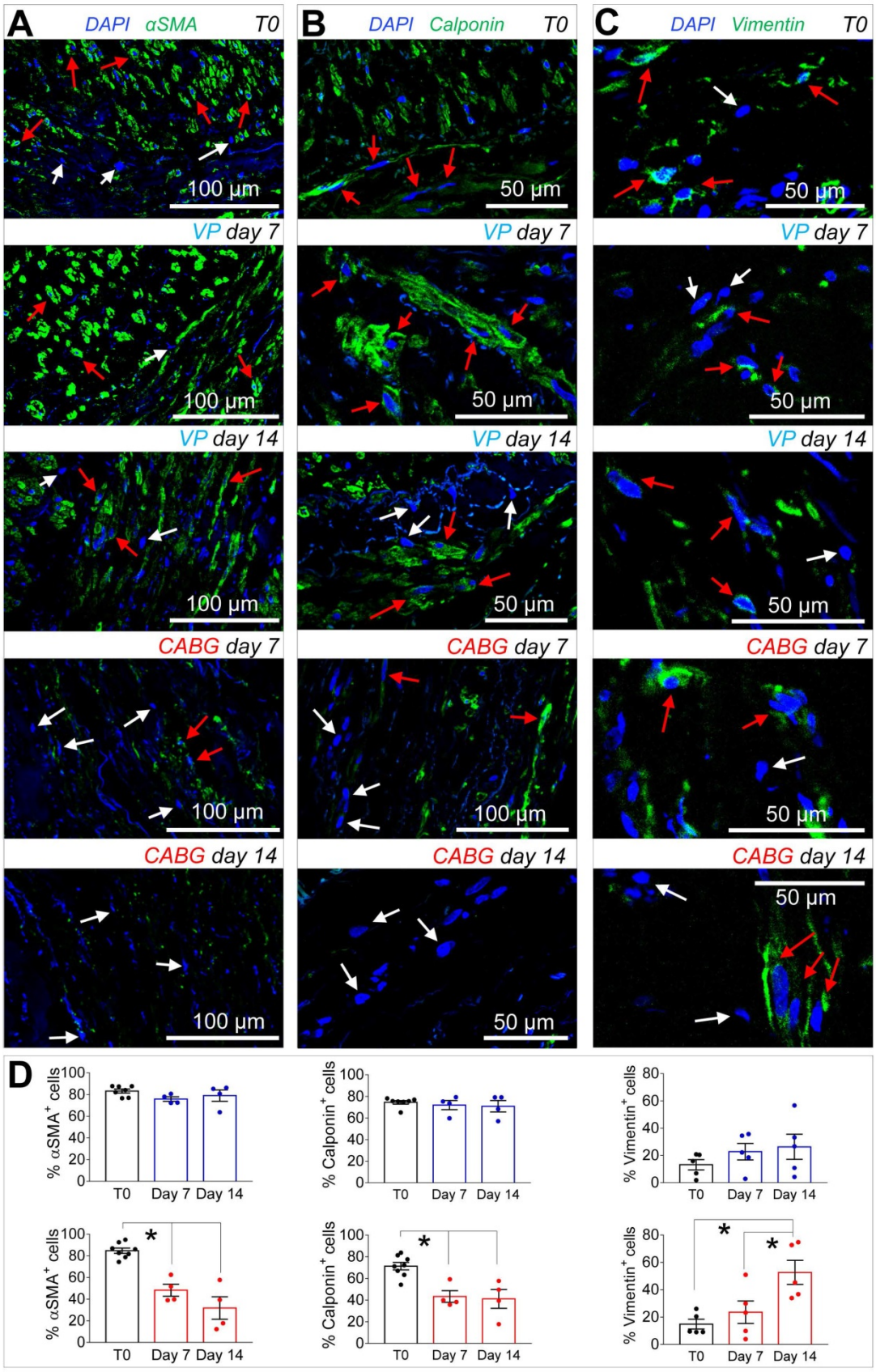

Figure 3. (A-C) Confocal microscopy images of transversal sections of native SVs (T0) and SVs exposed to venous perfusion (VP) or coronary flow (CABG) for 7 and 14 days stained with antibodies recognizing contractile (αSMA, Calponin) and secretory (Vimentin) SMCs markers. Red arrows indicate cells expressing the indicated markers, while the cells indicated by white arrows are marker$^-$ cells. (D) Quantification of the marker$^+$ cells expressed as a percentage of the total nuclei count present in the SV medial layer. Data are presented per treatment groups with blue bars indicating VP and red bars indicating CABG. * indicate $P < 0.05$ by one-way ANOVA with Newman-Keuls post-*hoc* comparison. Bar graphs represent mean and SE.

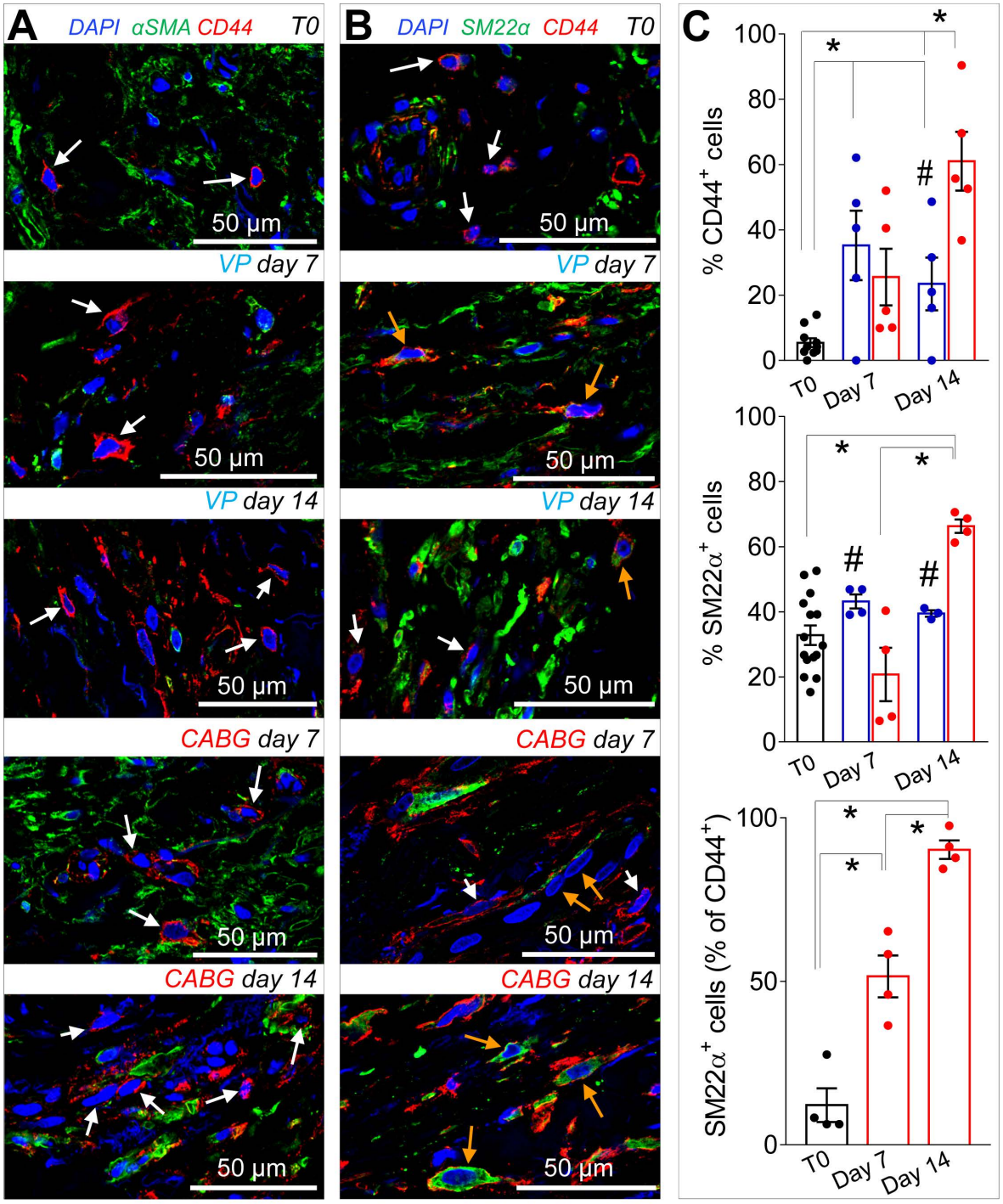

Figure 4. (A-B) Low and high magnifications of confocal images of SV tissue sections stained with CD44 with αSMA, (A) or SM22α (B) antibodies. While expression of αSMA was independent of that of CD44 (white arrows) a staining overlapping of CD44⁺ and SM22α⁺ (orange arrows) was observed especially in CABG samples at day 14 of stimulation. (**C**) Quantification of single marker⁺ cells or SM22α⁺/CD44⁺ cells in the medial layer of SV conduits exposed to venous perfusion or coronary flow revealed a sharp increase in double positive cells in the CABG conditions. * indicate $P < 0.05$ by one-way ANOVA with Newman-Keuls comparison tests; # indicate $P < 0.05$ by unpaired Student's tests at the corresponding time points between the two treatments. Bar graphs represent mean and SE.

In order to find a relationship between the phenotypic switch occurring in SMCs and the observed activation and presence of CD44⁺ cells, we performed a secretome analysis of proteins released in the culture medium by mechanically strained SMCs using a mass spectrometry-based approach. This indicated the matricellular protein Thrombospondin-1 (TSP-1) [28] as a factor released at high levels both at 24 and 72 h of mechanical stimulation (Table S2). Mass-spec data were validated in independent biological replicates using IF and ELISA tests, which confirmed TSP-1 release from SMCs (Figure 6C). Interestingly, Western analysis of the protein extracts revealed a decrease of the intracellular content of

TSP-1 in mechanically stimulated SMCs (Figure 6C). Altogether these data indicate that mechanical strain induces release of TSP-1 from intracellular stores and a concomitant upregulation at transcriptional level, thus identifying *TSP-1* as mechano-responsive gene. Finally, we performed immunohistochemistry and Western blotting analyses on tissue sections and protein extracts of samples treated with VP or CABG flow. This clearly showed a specific elevation of TSP-1 in the intima and media compartments of CABG-stimulated *vs.* VP and control SVs (Figure 6D-E). Immunofluorescence staining with anti-TSP-1 and -SM22α antibodies indicated the presence of TSP-1$^+$ cells with or without co-expression of the early SMCs marker in CABG-treated samples (Figure S8).

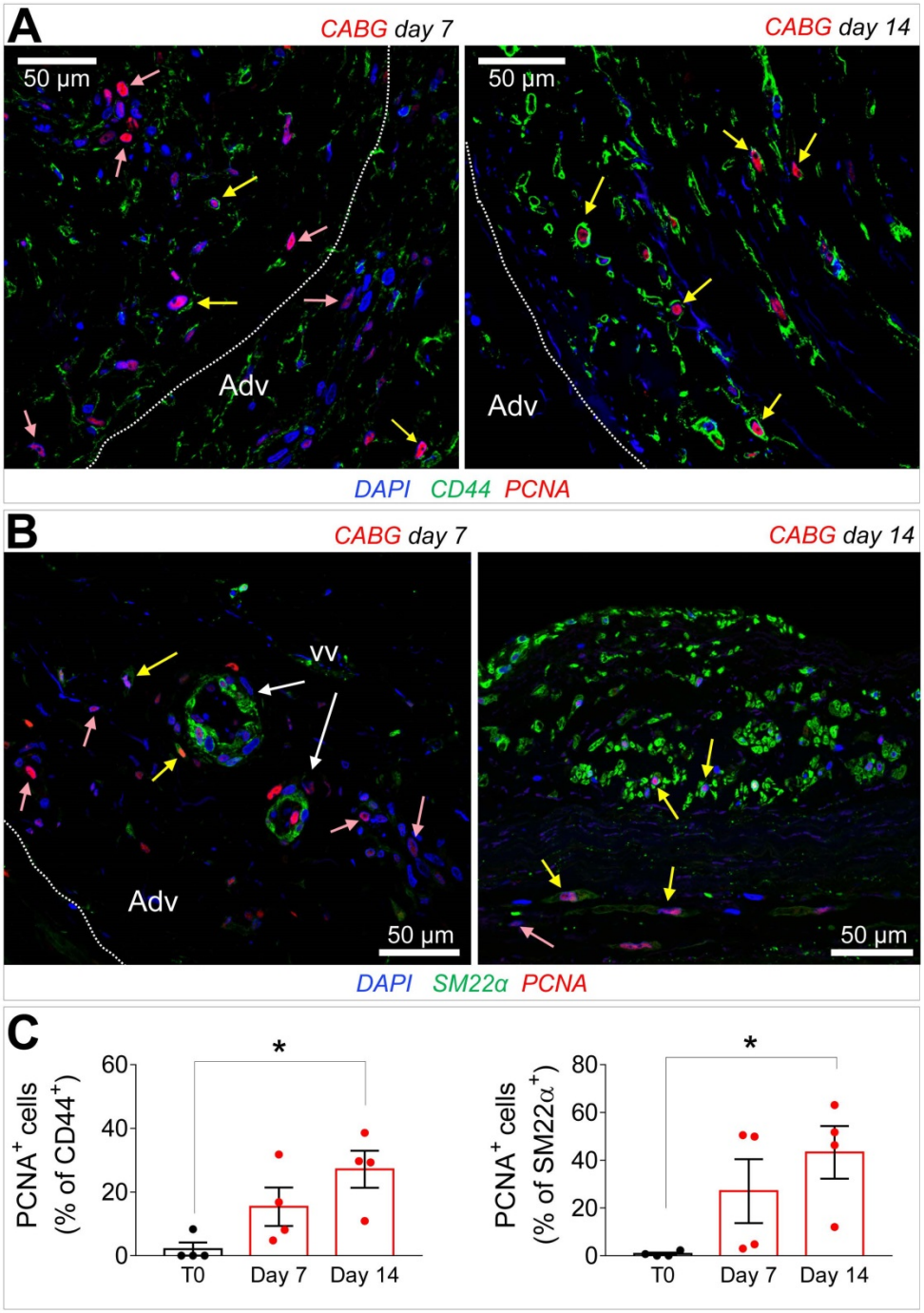

Figure 5. (A-B) Immunofluorescence staining of CABG-treated SV conduits sections with PCNA marker in conjunction with CD44 (A) or SM22α (B). PCNA$^+$ cells co-expressing (yellow arrows) or not co-expressing (rose arrows) the mesenchymal and the SMC markers were localized in the adventitia (Adv) at 7 days also in association with the *vasa vasorum* (VV) Dotted lines indicate the position of the external elastic lamina. (C) Quantification of CD44$^+$/PCNA$^+$ and SM22α$^+$/PCNA$^+$ cells in the medial layer. * indicate $P < 0.05$ by one-way ANOVA with Dunnett's post hoc comparison test. Bar graphs represent mean and SE of observations.

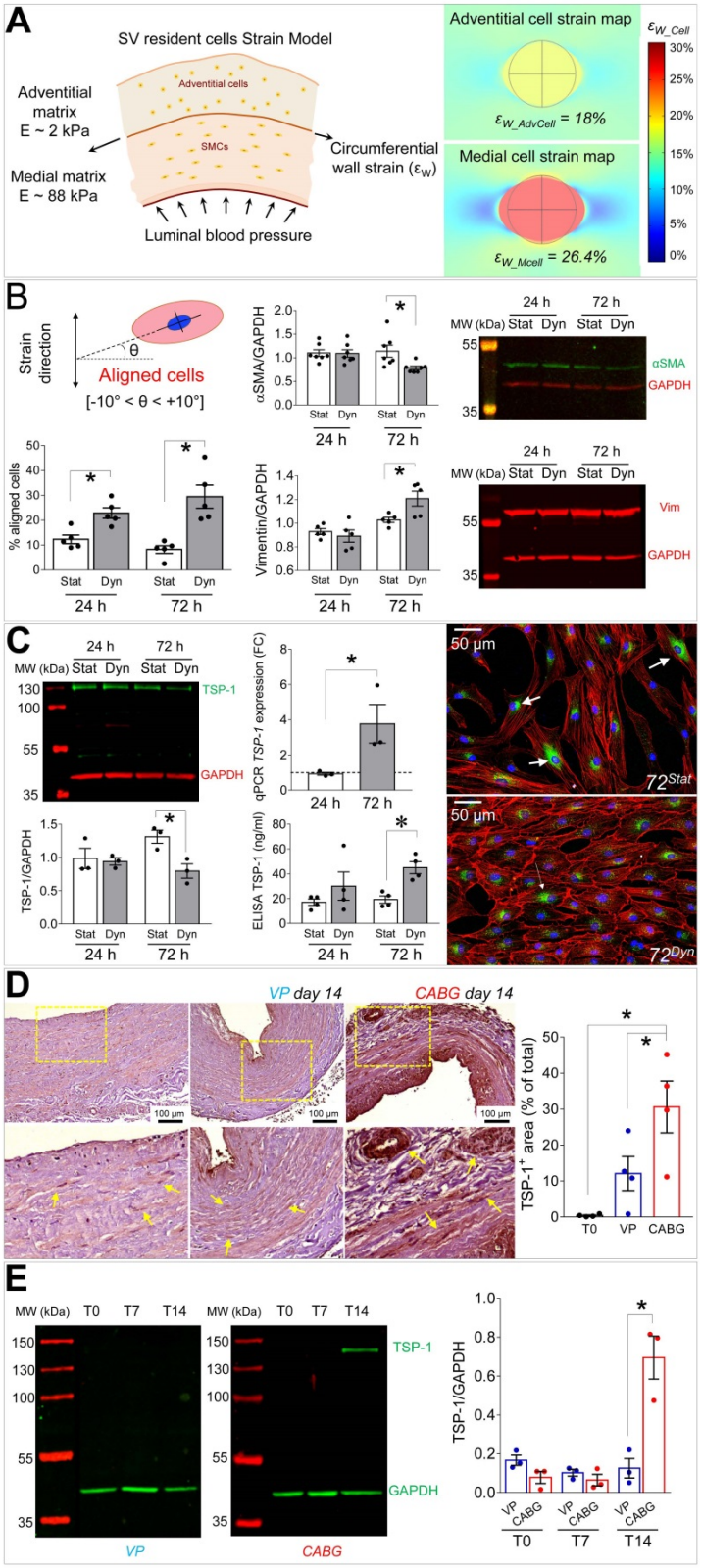

Figure 6. (A) On the left side of the panel, a schematic of the structural components, the stiffness characteristics (expressed as Young's modulus, E [kPa]) and the circumferential wall strain (ε_W) employed to compute cell stretching experienced by cells in the adventitial and in the medial layer when coronary blood pressure is applied. On the right side of the panel it is represented the predicted cell deformation maps in the medial (ε_{W_Mcell}) and adventitial ($\varepsilon_{W\_AdvCell}$) layers, as a result of the circumferential wall strain. (B) Results of 10% cyclic stretching on orientation of SV-SMCs (see scheme showing the procedure adopted to calculate cellular orientation above the bar graph on the left); modulation of αSMA and Vimentin by Western blot analysis (right). (C) Western blotting and IF (left side and right side, respectively) of TSP-1 into mechanically stimulated cells; ELISA tests of TSP-1 release in the medium. *TSP-1* gene expression analysis by Q-RT-PCR (central part of the panel). (D) TSP-1 immunohistochemistry in VP and CABG-stimulated SV samples. Statistical analysis indicated a significant difference in signal intensity at day 14 in CABG (red bars) *vs.* VP (blue bars) and T0 (white bars) samples. (E) Western blotting analysis of whole protein extracts from SV samples. As shown in the quantification graph, CABG-treated samples at day 14 (red bars) underwent a dramatic upregulation of TSP-1 compared with VP samples (blue bars) and earlier CABG time points, or controls. * indicate $P < 0.05$ by, (B, C) paired t-test, (D) one-way ANOVA with Newman-Keuls multiple comparison post-*hoc* test and unpaired t-test (E). Bar graphs represent mean and SE of observations.

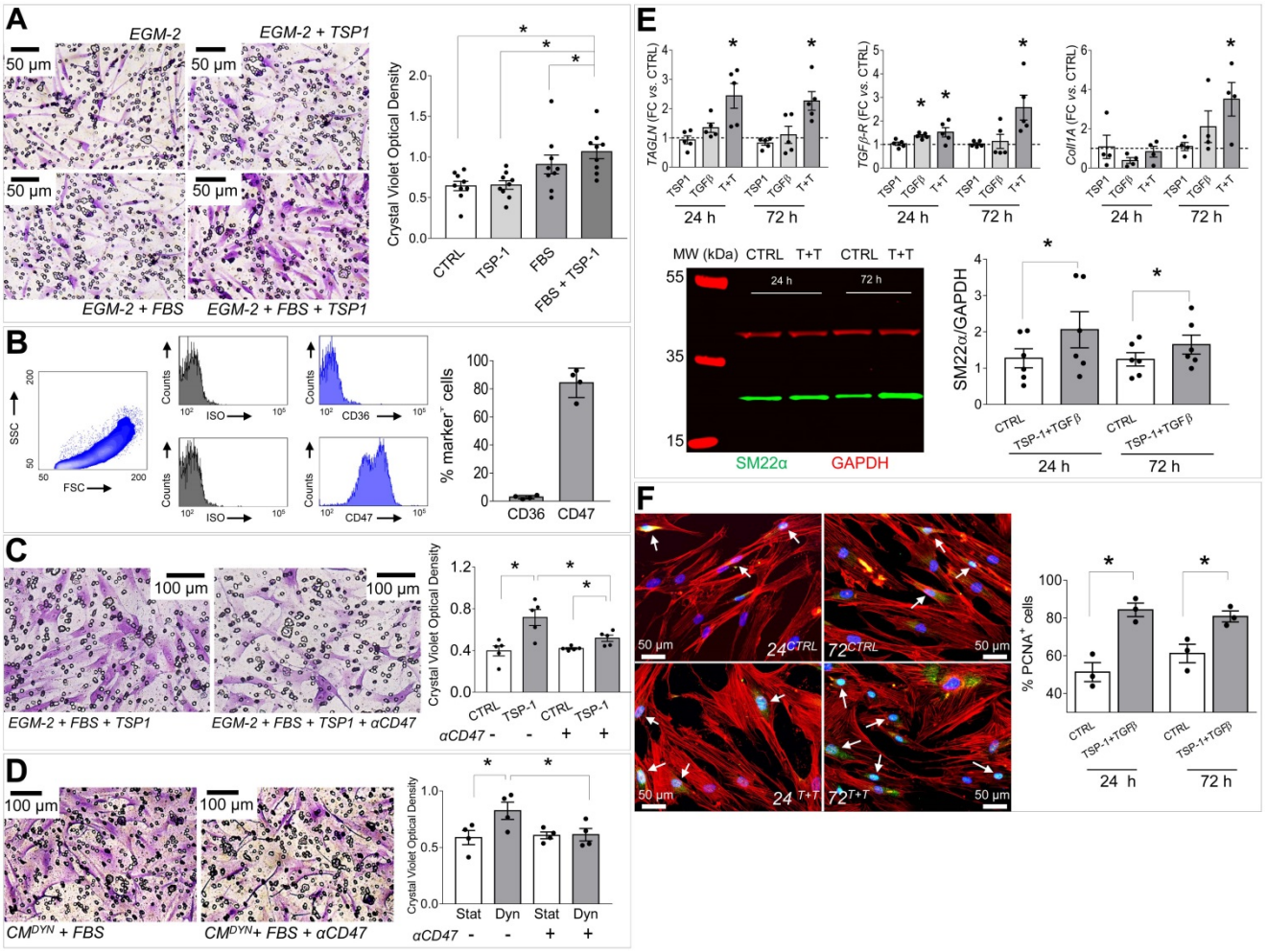

Figure 7. (A) SVPs transwell migration assay; micrographs show the cells that migrated through the membrane pores stained with Crystal Violet (purple color). Bar graph indicates quantification of the Crystal Violet optical density (see methods). * indicate $P < 0.05$ by one-way ANOVA (repeated measures) with Newman-Keuls multiple comparison post hoc test. (B) FACS analysis of the main TSP-1 receptors in human SVPs (n = 4). (C-D) Inhibition of SVPs migration against recombinant TSP-1 (C) and strained SMCs conditioned medium (D) by CD47 blocking antibody. * in both panels indicate $P < 0.05$ by paired student's t-test. (E) Effect of TSP-1/TGF-β treatment on SVPs phenotype. Q-RT-PCR analysis of *TAGLN* (SM22α), *TGFβR*, *Col1A* genes expression (upper). Data are represented as fold change (FC = $2^{-\Delta\Delta CT}$) *vs.* untreated cells cultured for the same amount of time (dotted line). * indicate P < 0.05 by paired t-test performed on ΔCT values. Western blotting analysis of SM22α protein expression (lower). * indicates P < 0.05 by paired t-test. (F) Effect of TSP-1/TGF-β treatment on SVPs proliferation (PCNA immunofluorescence, green). * indicate $P < 0.05$ by paired t-test. Bar graphs represent mean and SE of observations.

TSP-1 induces migration of SV adventitial progenitor cells

The human SV adventitia contains progenitor cells with pericyte characteristics, the so-called saphenous vein progenitors (SVPs) [20]. These cells are characterized by CD44 as well as other fibroblast/stromal cells markers (Figure S9) [26], and may represent a potential source of cells participating to SV graft pathologic evolution by differentiating into myofibroblasts and SMCs [12]. In order to correlate the mechanical-dependent TSP-1 regulation in the SV wall and activation/recruitment of CD44⁺ cells, we performed migration assays in Transwells (Figure 7A). Results showed that TSP-1 elevated the migration of the cells compared to serum only. As established in literature, TSP-1 exerts its cellular functions through specific receptors [28]. We therefore investigated the expression of TSP-1 receptors in SVPs using specific antibodies for CD36 and CD47, and this highlighted a high CD47 expression level (Figure 7B). To substantiate the role of TSP-1 on SVP migration, we treated cells with a blocking CD47 antibody in migration assays against the protein (Figure 7C) or the stretched SMCs conditioned medium (Figure 7D); in both cases, treatment with the antibody inhibited SVPs migration.

Integration of mechanosensing- and humoral-driven pathways in pleiotropic SVPs responses in saphenous vein graft failure

Taken together, the previous data suggested that CD44⁺/SM22α⁺ cells growing in SV conduits exposed to coronary mechanics are actively recruited from the adventitia where they initially reside; conversion from contractile to synthetic SMCs due to circumferential strain component attracts these cells in the medial

layer through secretion of TSP-1 and CD47-mediated chemotaxis. To get further insights in this process, we reasoned that transitioning from the adventitia to the media could expose cells to a combination of stimuli resulting from TSP-1 and classical vascular *pro*-remodeling factors, such as TGF-β [29]. On the other hand, we already showed that arterial-mimicking pressure elevates the expression of TGF-β in the SV, and literature reported a crucial function of TSP-1 for TGF-β pathologic activation of cells with mesenchymal and smooth muscle cells phenotypes [30, 31]. In order to substantiate this hypothesis, we stimulated SVPs with TGF-β (10 ng/mL) and TSP-1 (50 ng/mL), alone or in combination, followed by analysis of SM22α, Collagen1, TGF-βR, and cell proliferation. Results showed an increase in the expression level of the SMC/myofibroblast differentiation markers (Figure 7E-S10) and proliferation (Figure 7F-S11) at both times in cells treated with the factors combinations. For a final confirmation of TSP-1 expression in failing of arterialized veins, we performed immunostaining with TSP-1 antibodies in sections of SV grafts transplanted into carotids in pigs [32]. As shown in Figure 8A-C, SV grafts underwent a significant thickening of the intima layer, which peaked at 90 days post-transplantation. Concurrently, an increased number of cells expressing TSP-1(Figure 8B-C) and of $SM22\alpha^+/CD44^+$ cells (Figure 8D) was observed in the wall of the implanted SVs.

Discussion

We and others have hypothesized an important role of hemodynamic forces in molecular programming of the SV graft disease [12]. On the other hand, the lack of platforms mimicking the peculiar flow/pressure pattern existing in the coronary circulation has prevented the identification of molecular pathways connected to alterations of SV mechanics directly in human samples. In the present investigation we filled this gap using a platform customized to maintain vessel viability and reproducing the hemodynamic conditions of the coronary circulation [18]. We found a major vessel remodeling effect consisting in, *i)* a substantial rearrangement of the intima and the media layers structure, *ii)* a major change in cell composition resulting from an early induction of apoptotic death in a significant portion of the SMCs, accompanied by a transition from a contractile to a synthetic phenotype of the surviving SMCs associated with TSP-1 release in the media, and *iii)* proliferation of a vessel-resident cell subset arising from the SV adventitia, characterized by expression of CD44 and SM22α, leading to a fibrotic-like response associated to TSP-1 release.

Coronary mechanics induce SMCs phenotypic transition toward a synthetic phenotype and growth of a myofibroblast-like cell population in the SV media

The first questions that we aimed to resolve was to define the structural rearrangement of the vessel wall subjected to CABG conditions and the cellular dynamics occurring in consequence of the coronary stimulation *vs.* the venous flow/pressure pattern.

As shown in Figures 1, S1 and S2, under CABG conditions, the SV wall underwent a consistent thinning with reduction of the overall media thickness. Interestingly, the coronary-like stimulation was not associated to intima growth, while VP-stimulated vessels (analogous to the conventionally accepted SV culture method) exhibited significant intima thickening at day 14. This result, although contra-intuitive, is in line with observations performed in SV CABGs explanted *post mortem* showing narrowing of the vein wall and absence of intima hyperplasia at early times after implantation [33]. It further supports the hypothesis, already made in two other previous publications from our groups [18, 25], that the SVs contain a certain degree of damage before the culture that depends on surgical manipulation (e.g. interruption of collateral vessels, partial removal of the adventitia). In support of this hypothesis is, finally, the finding that TUNEL staining showed a similar level of apoptotic cells, especially at 7 days of culture, irrespective of the flow pattern (Figure 2).

IF data indicated that coronary mechanics induced synthetic SMCs phenotype, with a decrease in αSMA and Calponin and a parallel increase in Vimentin in the media layer (Figure 3). This is consistent with observations performed in animal models, in which medial SMCs lose contractile markers in favor of a synthetic phenotype [34, 35]. It is interesting to note that while disappearance of cells with contractile markers peaked at day 7, a consistent increase in $Vimentin^+$ cells occurred at day 14 of CABG stimulation. Thus, the shift in SMCs phenotype in the media was likely an effect of the adaptation of the cells surviving the early apoptotic peak to the new mechanical conditions. This conclusion is in line with reported differences in biological responses of synthetic SMCs to mechanical strain compared to their contractile counterparts [36]. The different response of these cells in the CABG mechanical condition may be finally part of the TSP-1-mediated pathway, given the reported protective effects from apoptosis of TSP-1/CD47 interactions in SMCs [37].

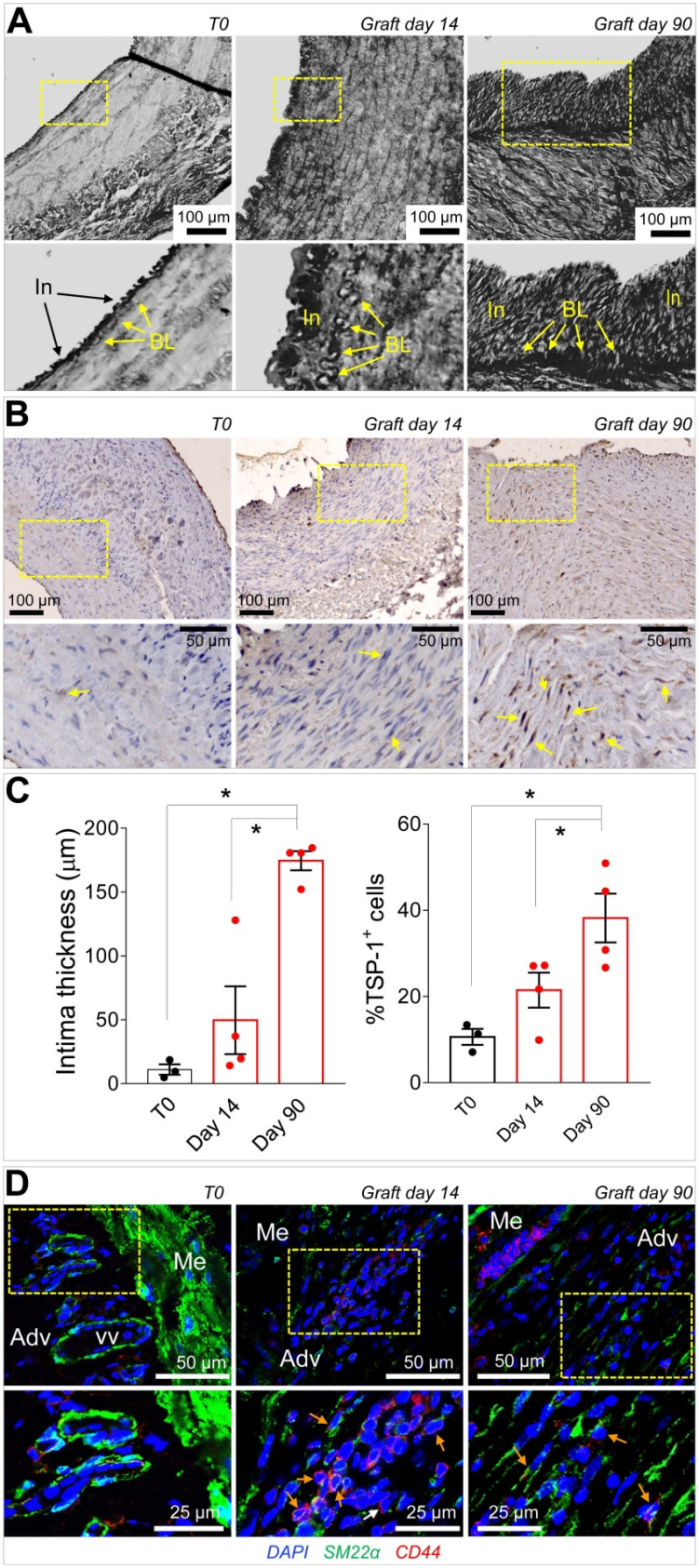

Figure 8. (A) Low and high magnifications (zones enclosed in the yellow areas) of transversal sections of porcine SV grafts before, and after 14 and 90 days *in vivo* arterialization. Yellow arrows indicate the intima basal lamina (BL). (B) Low and high magnifications (zones enclosed in the yellow areas) of section stained with anti TSP-1 antibody. Yellow arrows indicate TSP-1$^+$ cells. (C) Quantification of intima thickening and of TSP-1$^+$ cells. (D) Staining with antibodies directed against SM22α and CD44 of control (T0) and *in vivo* arterialized (day 14; day 90) SV in pigs. In the high magnifications on the bottom (correspondent to the zones enclosed in the yellow areas), orange arrows indicate cells expressing the two markers. * indicate $P < 0.05$ by one-way ANOVA with Newman-Keuls post-hoc test. Bar graphs represent mean and SE of observations.

Our immunofluorescence analyses of the SV wall revealed that in CABG condition, the vascular wall was repopulated by cells expressing the mesenchymal marker CD44 and early SMC marker SM22α. Due to marker overlapping between these strictly associated cell types, and the absence of methods to perform lineage-restricted cell tracking in the human tissue, it is at present not possible to conclude definitively whether these cells derive from direct activation of pre-existing $CD44^+/SM22\alpha^+$ SMCs or of progenitors with pericyte characteristics associated to *vasa vasorum*[38]. CD44 is, in fact, the ligand for hyaluronan, and it is involved in cell-cell/cell-matrix interactions in SMCs, myofibroblasts and inflammatory cells. This glycoprotein has been associated with SMCs differentiation [39], and high levels of CD44 have been associated with cell migration, injury-induced remodeling and fibrosis [27, 40]. SM22α/Transgelin is a F-Actin associated protein expressed in smooth muscle cells and fibroblasts, whose control has been recently associated to cell mechano-transduction [41]. Interestingly, in unstimulated samples $SM22\alpha^+/CD44^+$ cells were found almost uniquely in the adventitia in the *vasa vasorum* region, from where they appeared to invade the media at the later time point, especially in CABG condition (Figure S3, Figure 5). This finding is suggestive of a two-step adventitial cells recruitment process consisting of, at first, activation in the adventitia and, thereafter, active migration/proliferation in the media. Although these results are in contrast with findings obtained by passive culturing of SV vein rings (where there is no intervention of mechanical forces, Figure S1-S2) [23], they confirm findings in real CABGs explanted *post mortem*, where no intima hyperplasia was observed up to one month after implantation [33] and previous results obtained in our laboratory showing a structural rearrangement of *vasa vasorum* in response to hypoxia or mechanical injuries [19, 25]. Furthermore, they are in line with studies showing the contribution of adventitial progenitors to vein graft failure in animal models of vein arterialization [24].

A matricellular pathway mediated by Thrombospondin-1 accounts for activation of resident myofibroblast-like cells in SVs exposed to coronary mechanics

Cell sensitivity to mechanical cues is becoming more and more relevant for the progression of chronic fibrotic diseases as a fundamental part of damage repair process [42, 43]. Our *in silico* modelling of the cell strain in the two main layers of the SV wall predicted a particularly elevated level of mechanical stress for SMCs in the media (particularly those arranged in the circumferentially arranged bundles) (Figure 6). It was therefore crucial to expose these cells directly to cyclic mechanical stress *in vitro* and assess existence of signals secreted by these cells potentially involved in activation of adventitial resident cells. Given that *in vivo* mechanical stress sensed by these cells has a major uniaxial component [12], we performed a stimulation protocol along a unique direction with a 10% deformation level. Although this protocol led cells to experience a nominal deformation level lower than the maximal predicted by the model in the SV wall, we reasoned that mechanical forces in the real tissues is sensed by cells with a complex dynamics involving partial absorption by surrounding matrix due to its viscoelastic properties, while in the 2D condition cellular deformation occurs through direct transmission of elastic forces to cytoskeleton by the focal adhesion complexes [44]. The choice of a mass spectrometry approach to analyse the secretome of strained SMCs was made to not restrict our search for possible paracrine factors only on growth factors and chemokines that have been classically involved in progression of VGD, but also on the potential role of secreted proteins such as ECM components or matrix remodeling enzymes [29]. On the other hand, recent investigations by global proteomic profiling have disclosed new roles for ECM/matricellular vascular composition changes in early remodeling responses after injury [45]. Our secretomic analysis revealed TSP-1 as the factor more robustly released in the conditioned medium by SMCs subjected to mechanical stress. The role of TSP-1, and in a more general view, of members of the Thrombospondin family, have been so far connected to various effects on SMCs and vascular cells, such as focal adhesion kinase function, ERK1/2, p38 and CD44 regulation, migration, proliferation and arterial remodelling [46], but never specifically linked to VGD. This is important, especially in the view of recent evidences showing the susceptibility of TSP-1 expression/function to mechanosensitive control in formation of aortic aneurysm [47] or in disturbed flow-dependent arterial stiffening [48]. Although the objective of the present study was not to establish links between the response to mechanical cues and TSP-1 secretion by SV-SMCs, or to unveil the identity of mechanotransduction-dependent machineries controlling *TSP-1* gene expression at transcriptional level, it was remarkable to observe a sustained release of this factor specifically in the medial layer of CABG-stimulated human vessels (Figure 6, Figure S8), or in *in vivo* arterialized SV grafts (Figure 8). Together, these evidences support the hypothesis that release of TSP-1 in the vascular wall by SMCs is a damage response caused by SMCs mechanical stress

linked to the altered vessel flow dynamics, and potentially activating/recruiting adventitial cells with a myofibroblast phenotype.

Inspired by the vision of a mechano-paracrine mechanism involving TSP-1 in SV remodeling process, we finally established a mechanism for activation of adventitial cells in SV graft pathophysiologic process. Even if these cells have been extensively characterized for their vascular regeneration potential [20], the expression of several markers in common with mesenchymal cells such as CD105, CD90 and CD44 (Figure S9) suggests a specific vascular pathophysiologic role [38]. In our cell migration setting we observed a chemotactic effect of TSP-1 on SVPs. This effect was specific and involved CD47, one of the common TSP-1 receptor, expressed at high levels in these cells (Figure 7). Furthermore, compared to the treatment with the single factors, the combined treatment with TSP-1 and TGF-β increased SVPs maturation toward a SMC/myofibroblast phenotype, as shown by results of *TAGLN1*, *TGFBR1* and *Col1A* genes expression, SM22 protein expression and proliferation (Figure 7, Figure S10-S11). Taken together, these results support a multiple role of TSP-1 in activating myofibroblast-like progenitors migration from adventitial *vasa vasorum* and in modulating the latent TGF-β signaling, to promote maturation and proliferation of these cells in the media [49]. This hypothesis is in line with previous observations performed in mesenchymal progenitors [30] and SMCs [46], and establishes a new function of TSP-1 in early mechanical-dependent modification of matricellular composition in human SV grafts. The potential of our mechano-dependent graft pathology model was finally tested in the SV into carotid interposition in pigs, a widely accepted, robust and reproducible large animal system to assess vein arterialization. Data obtained in this system (Figure 8) confirmed the overexpression of TSP-1 and in the vascular wall of transplanted SVs and a similar dynamics of SM22α/CD44$^+$ in the adventitial region, and this correlated with neointima accumulation.

In conclusion, our study unravels for the first time a molecular mechanism linking mechanical injury occurring in coronary SV grafts with programming of intima hyperplasia by a mechano-paracrine effect. While this evidence demonstrates the relevance of cell-based mechanosensing in fibrotic diseases of the cardiovascular system, it calls for more focused studies addressing the potential reduction of intima thickening, e.g. by treatments with peptides inhibiting the TSP-1 function to resolve the timely issue of venous CABGs occlusion [50].

Supplementary Material

Supplementary methods, figures, and tables.
http://www.thno.org/v10p2597s1.pdf

Acknowledgements

This work has been supported by Institutional (Ricerca Corrente, 5 per mille, M.P.) and an Italian Ministry of Health grant funding (Ricerca Finalizzata, RF-2011-02346867, MP, MS and PM). ACT is currently supported by a grant to Prof Paolo Madeddu by the Medical Research Council UK. ACT was supported by the British Heart Foundation (under the Chairs of Prof Gianni Angelini and Prof Andrew Newby) for some of the work performed during this study.

Competing Interests

The authors have declared that no competing interest exists.

References

1. Parang P, Arora R. Coronary vein graft disease: pathogenesis and prevention. Can J Cardiol. 2009; 25: e57-62.
2. Wallitt EJ, Jevon M, Hornick PI. Therapeutics of vein graft intimal hyperplasia: 100 years on. Ann Thorac Surg. 2007; 84: 317-23.
3. Owens CD. Adaptive changes in autogenous vein grafts for arterial reconstruction: clinical implications. J Vasc Surg. 2010; 51: 736-46.
4. Li Y, Zheng Z, Hu S. The Chinese coronary artery bypass grafting registry study: analysis of the national multicentre database of 9248 patients. Heart. 2009; 95: 1140-4.
5. Gasper WJ, Owens CD, Kim JM, Hills N, Belkin M, Creager MA, et al. Thirty-day vein remodeling is predictive of midterm graft patency after lower extremity bypass. Journal of Vasc Surg. 2013; 57: 9-18.
6. Westerband A, Gentile AT, Hunter GC, Gooden MA, Aguirre ML, Berman SS, et al. Intimal growth and neovascularization in human stenotic vein grafts. J Am Coll Surg. 2000; 191: 264-71.
7. Tsui JCS, Dashwood MR. Recent Strategies to Reduce Vein Graft Occlusion: a Need to Limit the Effect of Vascular Damage. Eur J Vasc Endovasc Surg. 2002; 23: 202-8.
8. Hassantash S-A, Bikdeli B, Kalantarian S, Sadeghian M, Afshar H. Pathophysiology of Aortocoronary Saphenous Vein Bypass Graft Disease. Asian Cardiovasc Thorac Ann. 2008; 16: 331-6.
9. Majesky MW, Dong XR, Hoglund V, Daum G, Mahoney WM, Jr. The adventitia: a progenitor cell niche for the vessel wall. Cells Tissues Organs. 2012; 195: 73-81.
10. Thomas AC. Animal models for studying vein graft failure and therapeutic interventions. Curr Opin Pharmacol. 2012; 12: 121-6.
11. Ruiter MS, Pesce M. Mechanotransduction in Coronary Vein Graft Disease. Front Cardiovasc Med. 2018; 5.
12. Garoffolo G, Madonna R, de Caterina R, Pesce M. Cell based mechanosensing in vascular patho-biology: More than a simple go-with the flow. Vascul Pharmacol. 2018; 111: 7-14.
13. de Waard V, Arkenbout EK, Vos M, Mocking AI, Niessen HW, Stooker W, et al. TR3 nuclear orphan receptor prevents cyclic stretch-induced proliferation of venous smooth muscle cells. Am J Pathol. 2006; 168: 2027-35.
14. O'Callaghan CJ, Williams B. Mechanical Strain–Induced Extracellular Matrix Production by Human Vascular Smooth Muscle Cells: Role of TGF-β1. Hypertension. 2000; 36: 319-24.
15. Lüscher TF, Predel HG, Yang Z, Bühler FR, von Segesser L, Turina M. Implications of pulsatile stretch on growth of saphenous vein and mammary artery smooth muscle. Lancet. 1992; 340: 878-9.
16. Kona S, Chellamuthu P, Xu H, Hills SR, Nguyen KT. Effects of cyclic strain and growth factors on vascular smooth muscle cell responses. Open Biomed Eng J. 2009; 3: 28-38.
17. Schad JF, Meltzer KR, Hicks MR, Beutler DS, Cao TV, Standley PR. Cyclic strain upregulates VEGF and attenuates proliferation of vascular smooth muscle cells. Vasc Cell. 2011; 3: 21.
18. Piola M, Ruiter M, Vismara R, Mastrullo V, Agrifoglio M, Zanobini M, et al. Full Mimicking of Coronary Hemodynamics for Ex-Vivo Stimulation of Human Saphenous Veins. Ann Biomed Eng. 2017; 45: 884-97.
19. Prandi F, Piola M, Soncini M, Colussi C, D'Alessandra Y, Penza E, et al. Adventitial vessel growth and progenitor cells activation in an ex vivo culture

system mimicking human saphenous vein wall strain after coronary artery bypass grafting. PLoS ONE. 2015; 10: e0117409.
20. Campagnolo P, Cesselli D, Al Haj Zen A, Beltrami AP, Krankel N, Katare R, et al. Human adult vena saphena contains perivascular progenitor cells endowed with clonogenic and proangiogenic potential. Circulation. 2010; 121: 1735-45.
21. Worth NF, Rolfe BE, Song J, Campbell GR. Vascular smooth muscle cell phenotypic modulation in culture is associated with reorganisation of contractile and cytoskeletal proteins. Cell Motil Cytoskeleton. 2001; 49: 130-45.
22. Brioschi M, Lento S, Tremoli E, Banfi C. Proteomic analysis of endothelial cell secretome: A means of studying the pleiotropic effects of Hmg-CoA reductase inhibitors. J Proteomics. 2013; 78: 346-61.
23. McDonald RA, White KM, Wu J, Cooley BC, Robertson KE, Halliday CA, et al. miRNA-21 is dysregulated in response to vein grafting in multiple models and genetic ablation in mice attenuates neointima formation. Eur Heart J. 2013; 34: 1636-43.
24. Hu Y, Zhang Z, Torsney E, Afzal AR, Davison F, Metzler B, et al. Abundant progenitor cells in the adventitia contribute to atherosclerosis of vein grafts in ApoE-deficient mice. J Clin Invest. 2004; 113: 1258-65.
25. Piola M, Prandi F, Fiore GB, Agrifoglio M, Polvani G, Pesce M, et al. Human Saphenous Vein Response to Trans-wall Oxygen Gradients in a Novel Ex Vivo Conditioning Platform. Ann Biomed Eng. 2016; 44: 1449-61.
26. Klein D, Weißhardt P, Kleff V, Jastrow H, Jakob HG, Ergün S. Vascular Wall-Resident CD44+ Multipotent Stem Cells Give Rise to Pericytes and Smooth Muscle Cells and Contribute to New Vessel Maturation. PLoS ONE. 2011; 6: e20540.
27. Zhu H, Mitsuhashi N, Klein A, Barsky LW, Weinberg K, Barr ML, et al. The Role of the Hyaluronan Receptor CD44 in Mesenchymal Stem Cell Migration in the Extracellular Matrix. Stem Cells. 2006; 24: 928-35.
28. Resovi A, Pinessi D, Chiorino G, Taraboletti G. Current understanding of the thrombospondin-1 interactome. Matrix Biol. 2014; 37: 83-91.
29. de Vries MR, Simons KH, Jukema JW, Braun J, Quax PHA. Vein graft failure: from pathophysiology to clinical outcomes. Nat Rev Cardiol. 2016; 13: 451.
30. Belotti D, Capelli C, Resovi A, Introna M, Taraboletti G. Thrombospondin-1 promotes mesenchymal stromal cell functions via TGFβ and in cooperation with PDGF. Matrix Biol. 2016; 55: 106-16.
31. Stein JJ, Iwuchukwu C, Maier KG, Gahtan V. Thrombospondin-1-induced smooth muscle cell chemotaxis and proliferation are dependent on transforming growth factor-β2 and hyaluronic acid synthase. Mol Cell Biochem. 2013; 384: 181-6.
32. Thomas AC, Wyatt MJ, Newby AC. Reduction of early vein graft thrombosis by tissue plasminogen activator gene transfer. Thromb Haemost. 2009; 102: 145-52.
33. Stingl J, Musil V, Pirk J, Straka Z, Setina M, Sach J, et al. Vasa vasorum of the failed aorto-coronary venous grafts. Surg Radiol Anat. 2018; 40: 769-78.
34. Borin TF, Miyakawa AA, Cardoso L, De Figueiredo Borges L, Gonçalves GA, Krieger JE. Apoptosis, cell proliferation and modulation of cyclin-dependent kinase inhibitor p21cip1 in vascular remodelling during vein arterialization in the rat. Int J Exp Pathol. 2009; 90: 328-37.
35. Zhang WD, Bai HZ, Sawa Y, Yamakawa T, Kadoba K, Taniguchi K, et al. Association of smooth muscle cell phenotypic modulation with extracellular matrix alterations during neointima formation in rabbit vein grafts. J Vasc Surg. 1999; 30: 169-83.
36. Mantella L-E, Quan A, Verma S. Variability in vascular smooth muscle cell stretch-induced responses in 2D culture. Vasc Cell. 2015; 7: 7.
37. Mirochnik Y, Kwiatek A, Volpert OV. Thrombospondin and apoptosis: molecular mechanisms and use for design of complementation treatments. Curr Drug Targets. 2008; 9: 851-62.
38. Ferland-McCollough D, Slater S, Richard J, Reni C, Mangialardi G. Pericytes, an overlooked player in vascular pathobiology. Pharmacol Ther. 2017; 171: 30-42.
39. Simpson RML, Hong X, Wong MM, Karamariti E, Bhaloo SI, Warren D, et al. Hyaluronan Is Crucial for Stem Cell Differentiation into Smooth Muscle Lineage. Stem Cells. 2016; 34: 1225-38.
40. Li Y, Jiang D, Liang J, Meltzer EB, Gray A, Miura R, et al. Severe lung fibrosis requires an invasive fibroblast phenotype regulated by hyaluronan and CD44. J Exp Med. 2011; 208: 1459-71.
41. Liu R, Hossain MM, Chen X, Jin J-P. Mechanoregulation of SM22α/Transgelin. Biochemistry. 2017; 56: 5526-38.
42. Wolfenson H, Yang B, Sheetz MP. Steps in Mechanotransduction Pathways that Control Cell Morphology. Annu Rev Physiol. 2018.
43. Tschumperlin DJ, Ligresti G, Hilscher MB, Shah VH. Mechanosensing and fibrosis. J Clin Invest. 2018; 128: 74-84.
44. Jansen KA, Atherton P, Ballestrem C. Mechanotransduction at the cell-matrix interface. Semin Cell Dev Biol. 2017; 71: 75-83.
45. Suna G, Wojakowski W, Lynch M, Barallobre-Barreiro J, Yin X, Mayr U, et al. Extracellular Matrix Proteomics Reveals Interplay of Aggrecan and Aggrecanases in Vascular Remodeling of Stented Coronary Arteries. Circulation. 2018; 137: 166-83.
46. Moura R, Tjwa M, Vandervoort P, Cludts K, Hoylaerts MF. Thrombospondin-1 Activates Medial Smooth Muscle Cells and Triggers Neointima Formation Upon Mouse Carotid Artery Ligation. Arterioscler Thromb Vasc Biol. 2007; 27: 2163-9.
47. Yamashiro Y, Thang BQ, Shin SJ, Lino CA, Nakamura T, Kim J, et al. Role of Thrombospondin-1 in Mechanotransduction and Development of Thoracic Aortic Aneurysm in Mouse and Humans. Circ Res. 2018; 123: 660-72.
48. Kim CW, Pokutta-Paskaleva A, Kumar S, Timmins LH, Morris AD, Kang DW, et al. Disturbed Flow Promotes Arterial Stiffening Through Thrombospondin-1. Circulation. 2017; 136: 1217-32.
49. Murphy-Ullrich JE, Suto MJ. Thrombospondin-1 regulation of latent TGF-β activation: A therapeutic target for fibrotic disease. Matrix Biol. 2018; 68-69: 28-43.
50. Newby AC. Coronary vein grafting: the flags keep waving but the game goes on. Cardiovasc Res. 2013; 97: 193-4.

Coronary artery mechanics induces human saphenous vein remodeling *via* recruitment of adventitial myofibroblast-like cells mediated by Thrombospondin-1

Gloria Garoffolo[1, 2, †], Matthijs S. Ruiter[1,†], Marco Piola[3] , Maura Brioschi[4], Anita C. Thomas[5], Marco Agrifoglio[6], Gianluca Polvani[6], Lorenzo Coppadoro[3], Gaia Spinetti[7], Stefano Zoli[8], Claudio Saccu[8], Cristina Banfi[4], Gianfranco B. Fiore[3], Paolo Madeddu[5], Monica Soncini[3] and Maurizio Pesce[1,*]

Supplementary Material

Supplementary Methods

Ex vivo SV tissue stimulation

For bioreactor-based *ex vivo* stimulations, we employed exclusively SV segments obtained from patients undergoing CABG intervention (Table S1). To minimize the damage due to vessel manipulation in the surgery theatre, SVs employed for CABG implantation were harvested using a 'no touch' procedure[1, 2], which maintains almost integrally the adventitia. This is a standard procedure adopted by our cardiac surgery Teams to maintain patency in implanted SV grafts and maximize the clinical outcome. In order to maximize the vitality of the SV, the vessels were maintained hydrated in saline solution for the whole duration of the surgery. After vessels were released from the surgery room, they were stored in DMEM supplemented with 10% FBS, 1% L-Glutamine (L-Glut), 1% P/S (all by Lonza) at 4 °C until *ex vivo* tissue stimulation into bioreactors. As a quality checking process, they were measured in length and calibre at the two extremities. Indeed a variable calibre and length of the vessels may result into significant variability in the flow/pressure patterns experienced especially in the CABG. In any instance, SVs shorter than 5 cm and with a calibre < 5 mm were excluded from the study. Additionally, to avoid confounding boundary effects, the parts of the SVs considered to analyse the effect of mechanical forces were derived from the central portions (~3 cm in length) while the two extremities that were anchored to inlet/outlet of the stimulation systems by vessel loops were always discarded. SV segments were mounted in an EVCS mimicking coronary hemodynamics (CABG-like stimulation, luminal pressure: 80 - 120 mmHg; pulse frequency: 1 Hz; mean flow rate: ~150 mL/min)[3] or venous conditions as controls (VP, continuous luminal pressure: 5 mmHg; flow rate: 5 mL/min)[4, 5] and cultured for 7 or 14 days. DMEM supplemented with 10% FBS, 1% L-Glut, 1% P/S, and containing 3.5% Dextran (450000-650000 kDa, Sigma-Aldrich) was used to mimic blood-like viscosity of 3.2 cP in CABG-like stimulation. Medium (1/2 of the volume) was changed every 4 days. At the end of the stimulation period, SV samples were recovered. Portions of the stimulated SV were in part processed for histology and immunofluorescence and in part for proteomic analyses. Untreated tissue rings of each SV sample were fixed and snap-frozen upon arrival from the surgery theatre and stored to serve as baseline controls. In addition, to validate our venous control

condition, we determined intima thickness after conventional passive culture of SV segments, a common model of intimal hyperplasia described before[6-8], in which rings are cultured in medium (DMEM supplemented with 10% FBS, 1% L-Glut, 1% P/S) in the absence of mechanical stimuli.

Tissue morphometry and immunohistochemistry

Fixed tissue rings were embedded in paraffin and cut at 5 μm using a rotary microtome (Leica). Lumen perimeter and the distance of the outer part of the media were measured on sections stained with Masson's trichrome (MT) staining. Intima thickness was measured on sections stained with Weigert van Gieson (WvG, both from Bio-Optica Milano, Italy), and media thickness was determined as the difference between the two measurements. Digital images were acquired using a light microscope and dedicated software (AxioVision Bio Software, Carl Zeiss, Germany). For immunohistochemistry, after heat-induced epitope unmasking (citrate buffer, pH 6, 10 min) and quenching with hydrogen peroxide (0.6%, 20 min), nonspecific binding was blocked with bovine serum albumin (BSA 3%, 45 minutes, Sigma-Aldrich) and sections were incubated overnight with a primary antibody against TSP-1 (mouse anti-human A6.1, 2 μg/mL, Invitrogen). Subsequently, sections were incubated with a secondary antibody (rabbit anti-mouse IgG HRP, Invitrogen) for 1 h, after which colour was developed with diaminobenzidine (ImmPACT DAB, DBA, Italy) and nuclei were counterstained with hematoxylin. Apoptosis was determined on sections stained with the Deadend Colorimetric TUNEL System (Promega, Italy) according to the manufacturer's protocol and with a hematoxylin counterstain.

Tissue and Cell Immunofluorescence

Immunofluorescence (IF) staining for different markers was performed on sections after epitope unmasking and blocking with BSA (3%, 1 h). Sections were incubated overnight at 4 ˚C with primary antibodies and subsequently with appropriate AlexaFluor-conjugated secondary antibodies (Invitrogen) for 1 h at RT (Table S3). Cells positive for the different markers, counted in at least 3 fields per section, were expressed as percentage of total cells in the media. For cellular IF, after fixation with 4% paraformaldehyde (Sigma-Aldrich), cells were permeabilized for 30 min at RT with PBS containing 3% (w/v) BSA and 0.2% (v/v) Triton X-100 (AppliChem), followed by primary antibody incubation at 4 °C overnight. Negative control cells were incubated in a PBS solution containing 3% BSA. AlexaFluor labelled secondary antibodies were employed to detect primary antibodies. Digital images were obtained using an ApoTome fluorescence microscope or LSM-710 confocal scanning microscope (both Carl Zeiss, Germany). All measurements and quantifications were performed using ImageJ (version 1.46r, National Institutes of Health, USA). Analysis of 3 fields per section was found to be a good representation of markers expression in the whole tissue, based on the magnification used (10 X), and the average size of the sections. Four sections representative of four consecutive portions of the stimulated vessels were quantified for each condition and for each marker. Positive cells were counted in image files blinding the type of stimulation to the examiner. Marker^{+} cells were generally scored just when they clearly exhibited a complete staining around (membrane markers) or inside cytoplasm (cytoskeleton) or nuclei (proliferation markers). This staining pattern was visible only in tissue sections stained with the

primary/secondary antibody combinations and not in control staining that were included in every set of immunofluorescence labelling.

Isolation and culture of SV-derived cells

SVPs and SMCs for in vitro experiments were isolated from SVs of patients subjected to unilateral saphenectomy (Table S1). SVP isolation was performed as described previously [9]. In brief, the vein was mechanically minced and digested for 4 h at 37 °C with 3.7 mg/mL Liberase 2 (Roche). Remaining aggregates were removed through filtration with 70 µm and 40 µm cell strainer. $CD34^{POS}/CD31^{NEG}$ cells were isolated by magnetic bead-assisted cell sorting (MACS, Miltenyi Biotec). Cells were grown in a humidified atmosphere (95% air, 5% CO2) at 37 °C in Endothelial Growth medium (EGM-2) supplemented with 2% Fetal Bovine Serum (FBS) and 1% Penicillin/Streptomycin (P/S, all by Lonza). For SMCs isolation, after removing the external tissues, including the adventitia, veins were cut longitudinally to remove the endothelium by gentle scraping and then finally minced. Tissue fragments were incubated in Dulbecco Modified Eagle's Medium (DMEM) containing Liberase for enzymatic digestion. The resulting cells were cultured in DMEM supplemented with 10% FBS and 1% P/S. Passages between 4 and 6 were used for the experiments.

SVPs flow cytometry characterization

SV-derived progenitor cells were characterized by flow cytometry analysis. Cell suspensions were incubated with a combination of directly conjugated antibodies against CD31, CD36, CD44, CD47, CD90, CD105, CD140b and NG2 (all from BD Bioscience) for 15 minutes at room temperature (RT) in the dark. Data were acquired with FACSAria flow cytometry (BD Biosciences) and analyzed with flow cytometric sorting Diva software (BD Biosciences).

In silico modelling of strain responses in SV media and adventitia

An in-silico model was implemented with the aim of quantifying the deformation experienced by the cells embedded in different extracellular matrices, namely the adventitial layer or the medial layer. The cell was assumed as a 10 µm-diameter sphere embedded in an ECM volume. The cell and the ECM perfectly adhere at their interface. A 40 µm-edge cubic ECM volume was modelled around the cell, with two additional lateral extension volumes that were used to smooth the edge effects caused by the application of lateral displacements as the mechanical loading condition. The overall volume (ECM plus cell) was meshed with about ~ 230.000 tetrahedral elements. A linear elastic constitutive model was used for the materials representing the ECM and the cell. Young's moduli were set according to the literature: Young's moduli were set according to literature: 1 kPa for cells [10] 2 kPa for the adventitia (which was treated as a soft collagen matrix [11]) and 88 kPa for the media layer [12, 13]. Lateral displacements were applied to the lateral surfaces of the extension volumes, in such a way as to simulate a 16% strain for the cubic ECM volume. Such strain value was meant to represent the circumferential strain at which the vessel matrix is subjected when it is loaded with an arterial-like pressure. It was estimated by means of the Laplace law, considering blood pressure in the range 80-120 mmHg, a vessel diameter of 2.5-3 mm, a media thickness of 0.52 mm (as measured from histological slices of 9 SV samples),

and the media Young modulus of 88 kPa, under the assumption that the pressure load is supported entirely by the medial layer.

In vitro cell straining

To investigate the effect of isolated mechanical strain on cultured cells, SMCs were subjected to cyclic strain using the FlexCell Tension Plus FX-5000T system (Flexcell International Corp., Hillsborough, NC). Before cell seeding, six-well Uniflex plates were surface-coated with bovine fibronectin (10 µg/mL; Sigma- Aldrich) in PBS after covalent crosslinking with a crosslinking reagent (sulfosuccinimidyl 6-(4'-azido-2'-nitrophenylamino) hexanoate; Sulfo-SANPAH; Pierce) at 0.2 mg/mL in Hepes 50 mM (pH 8.5), photo-activated by exposure to UV-light (365 nm). Cells were seeded 10^5/well and allowed to attach overnight before beginning the uniaxial cyclic deformation protocol (0-10% deformation, 1 Hz frequency), for 24 and 72 h. Static controls were provided by seeding an equal amount of cells into the same FN-coated plates, keeping them under the same atmospheric conditions but without mechanical stimulation.

Western and ELISA analyses

Western blot analyses were performed according to standard procedures. Cells were lysed in a buffer containing 10 mM Tris-Cl, pH 7.4, 150 mM NaCl, 5 mM EDTA, 1% (v/v) Triton X-100, 1% (w/v) sodium deoxycholate, 0.1% (w/v) sodium dodecyl sulfate and 1% (v/v) protease and phosphatase inhibitor mixture (Sigma-Aldrich). Whole cell lysates were sonicated, centrifuged for 15 min at 14 000 g; cell supernatants were then collected. Proteins were quantified by BCA protein assay kit (Pierce Chemical Co). Cell lysates (30 µg per lane) were diluted in Laemli sample buffer, heated at 95 °C for 5 min, run onto 4-12% gradient SDS-polyacrylamide gels (Invitrogen), and transferred to nitrocellulose membranes. The blots were blocked with Tris Buffered-saline containing 5% (w/v) nonfat dried milk (AppliChem) at RT for 1 h. Overnight incubation at 4 °C with primary antibodies listed in Table S4 was performed to examine individual protein expression. Membranes were finally incubated with appropriate secondary antibodies for 20 min. Images were taken by LI-COR Odyssey and band densities were quantified using ImageJ software. An enzyme-linked immunosorbent assay (ELISA, #BMS2100, Invitrogen) was performed on conditioned medium of strained *vs.* control SMCs according to the manufacturer's instructions to detect the levels of human TSP-1. Calibration curves were prepared using purified standards for the protein assessed and curve fitting was accomplished by regression following the manufacturer's instructions.

mRNA analysis

Total RNA was extracted from cell lines using TRIzol (Invitrogen), quantified with NanoDrop-1000 spectrophotometer (Thermo Fisher Scientific) before integrity assessment with an Agilent 2100 Bioanalyzer (Agilent Technologies). Superscript III (Thermo Fisher Scientific) was used for reverse transcription. Quantitative real-time PCR analysis were performed with Power SYBR Green PCR Master Mix (Applied Biosystems) in an ABI 7900 Fast thermal cycler to detect *TSP-1*, *TAGLN*, *TGFβR*, *Coll1A* gene amplification products (primers details in Table S5). The reported expression levels were calculated relative to GAPDH

mRNA, used as an internal standard control. The fold change of the genes in strained condition vs. control samples was calculated as $2^{-\Delta\Delta CT}$ and the statistical analysis was done on the ΔCT values.

Mass spectrometry of culture supernatants

For the analysis of cell secretome by label-free mass spectrometry, the conditioned media were collected from strained or not-strained SMCs and processed as described [14, 15]. Quantitative label-free LC-MSE was performed on a hybrid quadrupole-time of flight mass spectrometer (Synapt-MS, Waters Corporation, Milford, USA) as previously described [16, 17]. The proteins were identified and quantified using Progenesis QIP for proteomics (v3.0, NonLinear dynamics, Newcastle upon Tyne, UK) with a human species-specific UniProt database (release 2017.1; 20,201 entries). For SVPs migration with static/dynamically cultured SMCs conditioned medium, the culture supernatant of 3 SMCs independent donors was pooled after ELISA test checking of TSP-1 and concentrated by lyophilizing/dialyzing. TSP-1 content of the resuspended CM was checked by ELISA before performing migration experiments.

SVP Migration assay

Migration capacity was measured by Transwell assays (Corning). SVPs (15,000) were seeded in EGM-2 without FBS in the upper part of a cell culture-chamber-insert system separated from the lower chamber by an 8 µm PET membrane. In the lower compartment, four conditions were assayed: EGM-2 without FBS (negative control), EGM-2 plus 10% FBS (positive control), EGM-2 plus recombinant human TSP-1 (experimental condition 1, 10 µg/mL, R&D Systems) and EGM-2 10% FBS plus TSP-1 (experimental condition 2, 10 µg/mL), or SMCs conditioned medium. After 24 h, non-migrating cells in the upper compartment were scrapped off with a cotton swab, while cells on the lower side of the membrane were fixed with 4% paraformaldehyde for 10 min and permeabilized with methanol for 20 min at RT. Migrated cells were then stained with 1% (w/v) Crystal Violet diluted in 2% (v/v) ethanol for 30 min and images were acquired with Axiovert 200M (Zeiss). For Crystal Violet quantification, the staining was solubilized with 2% (v/v) SDS and optical density (550 nm) was measured using Infinite M200 PRO reader (Tecan). To inhibit TSP-1-dependent migration, cells were incubated at 37 °C for 30 min in serum-free EGM2 in presence or absence of function blocking antibody to CD47 (clone B6H12, 20 µg/mL, Invitrogen) and its isotype control (IgG1, 20 µg/mL, Invitrogen) before subjecting them to the transwell assay.

In vivo porcine arterialization SV model

Anaesthesia was induced with intramuscular ketamine administration (0.1 mg/Kg). After endotracheal intubation, anaesthesia was maintained using halothane, the animals ventilating spontaneously throughout. A 12-15 cm of the left long saphenous vein was isolated using a ‘no touch’ technique[18-21], the vein divided and stored in iso-osmotic sodium chloride solution (containing 2 IU/mL heparin (CP Pharmaceuticals Ltd, Wrexham, UK) and 50 µg/mL-glyeryl trinitrate (Schwarz Pharma, Bucks, UK; room temperature) until required, to prevent spasm. The animal was heparinized by intravenous administration of 100 IU/Kg of heparin. Both common carotid arteries were exposed via longitudinal neck incisions medial to the

sternomastoid muscle. End-to-end interposition grafts were created in both common carotid arteries (using continuous 7-0 Prolene or Surgipro), with reversed 45°-bevelled 3 cm segments of saphenous vein replacing 45°-bevelled 1 cm excised segments of carotid artery. The proximal and distal anastomoses were approximately 4 cm apart. The order of performing the grafts and the site of insertion (left or right) were randomized between procedures and the vein segments. Neck and leg wounds were closed in layers, and the animals given antibiotic cover (ampicillin (200 mg amfipen (MSD Animal Health, UK) in sterile water i.m.) and appropriate levels of analgesia (buprenorphine (Vetergesic (Ceva Animal Health Ltd, UK) 15 μg/Kg i.m.), repeated as necessary). Animals were observed continually during recovery, which always took less than 1 h. Once recovered, the animals were inspected daily and fed a normal diet and given water ad libitum. Analgesia was continued as required, but no animal required additional antibiotic cover.

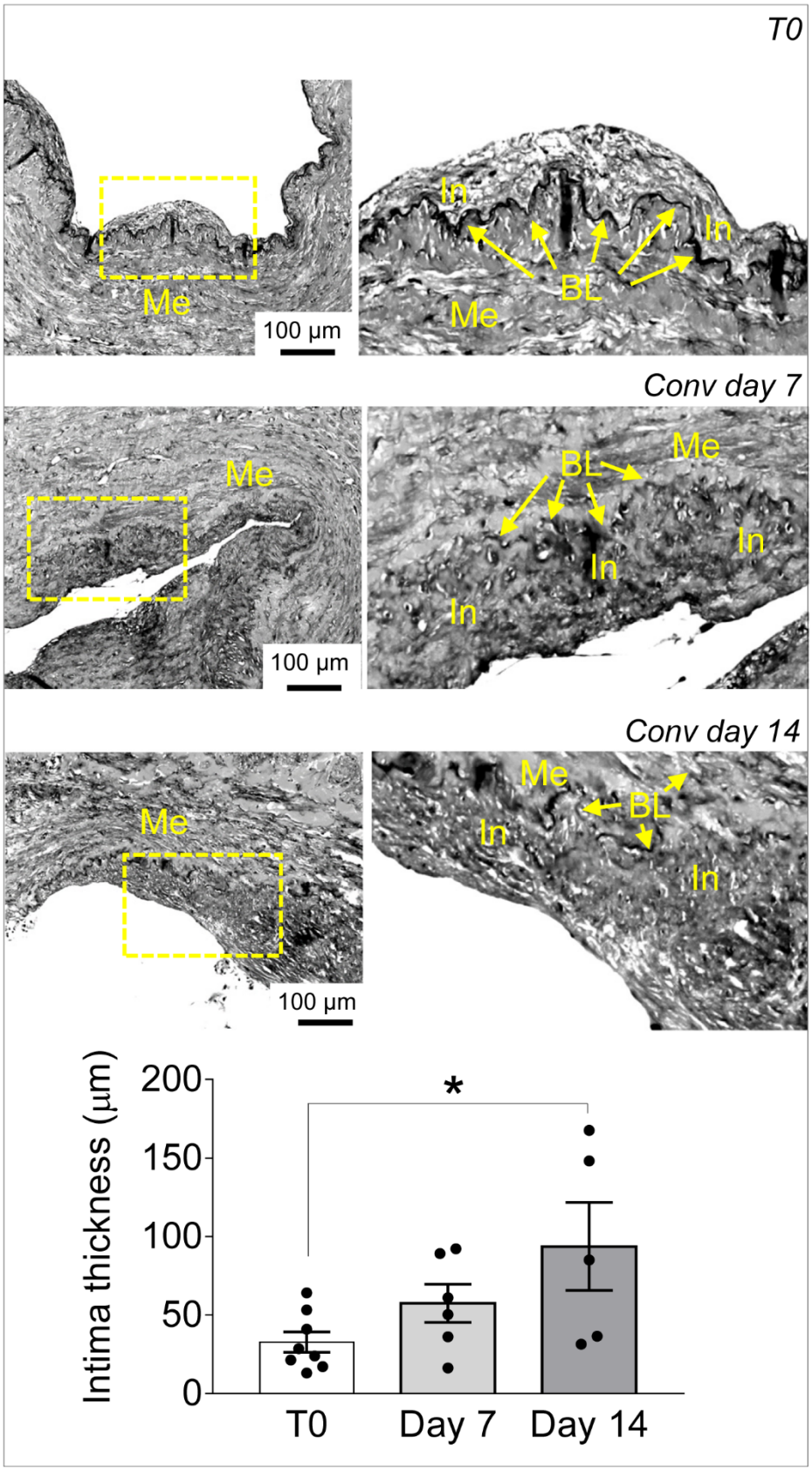

Figure S1. Low and high magnifications (zones enclosed in the yellow areas) of transversal sections of conventionally cultured SVs to show intima hyperplasia (IH) as demonstrated in the literature [22]. Yellow arrows indicate the basal lamina (BL), particularly evident in B/W pictures of Weigert van Gieson staining. Bar graph on the bottom shows quantitative evaluation of intima thickness at the indicated time points. *

indicates $P < 0.05$ by one-way ANOVA with Newman-Keuls multiple comparison post-hoc test. Me = Media; In = Intima. Bar graph represent mean and SE of observations.

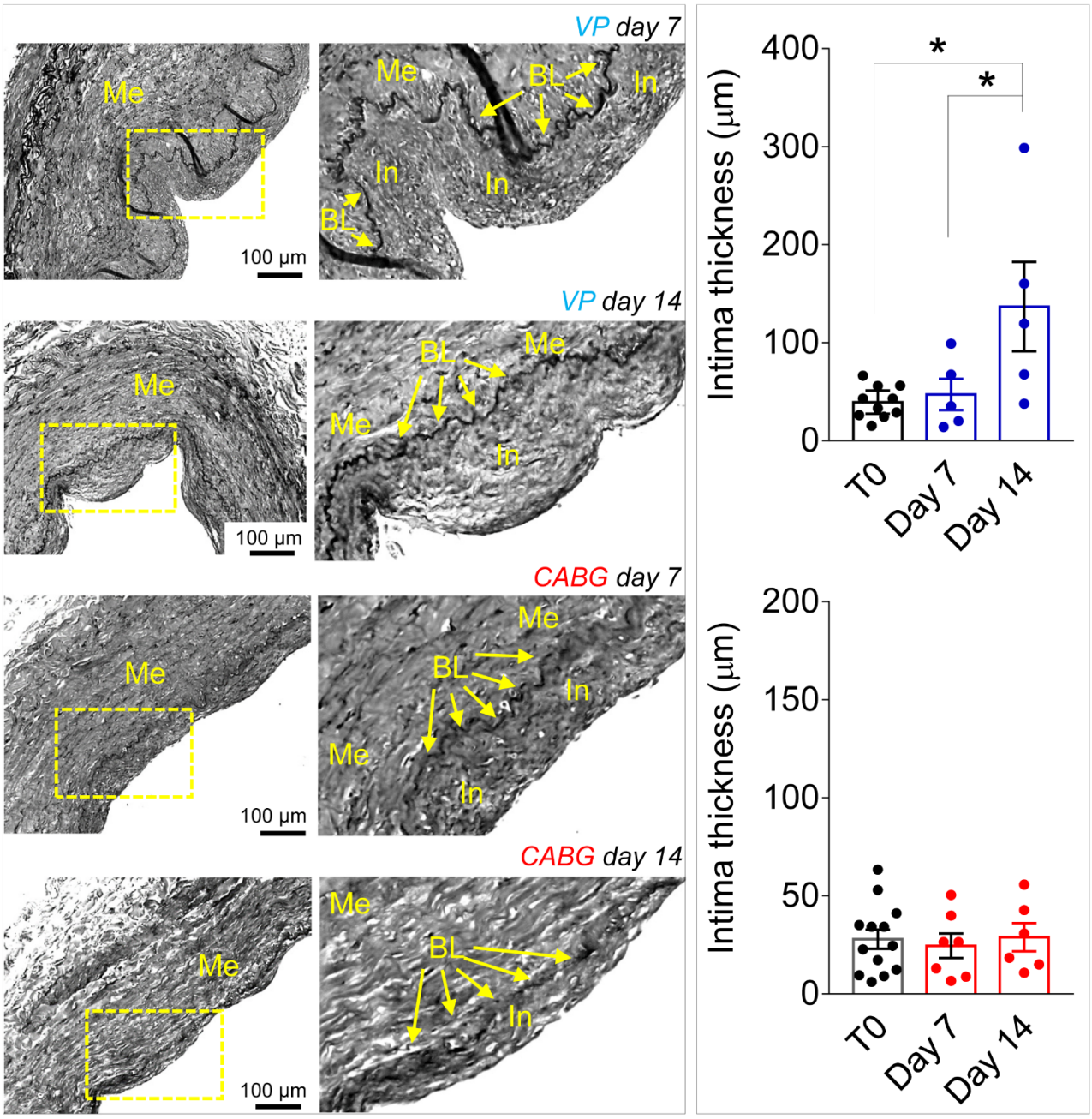

Figure S2. Low and high magnifications (zones enclosed in the yellow areas) of transversal sections of native SVs (T0) and SVs exposed to venous perfusion (VP) or coronary flow (CABG) for 7 and 14 days stained with Weigert van Gieson solution. Yellow arrows indicate the basal lamina (BL) evident in high contrast B/W pictures. Bar graphs on the right show quantitative evaluation of intima thickness at the indicated time points. * indicates $P < 0.05$ by one-way ANOVA with Newman-Keuls multiple comparison post-hoc test. Me = Media; In = Intima. Bar graphs represent mean and SE of observations.

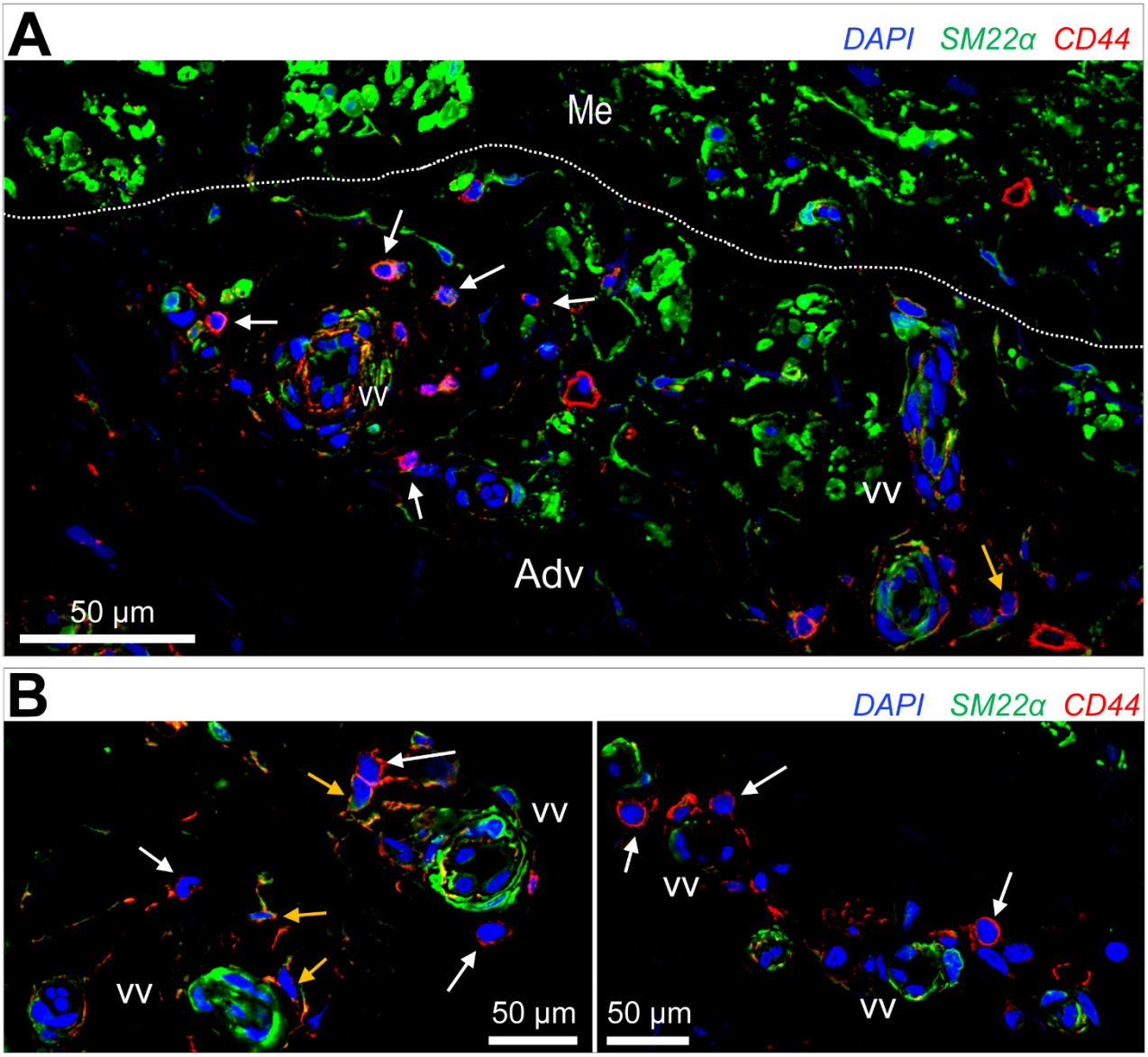

Figure S3. Low (A) and high (B) magnification of Control (T0) SV transversal sections stained with CD44 and SM22α antibodies. Note the localization of $CD44^+$ (white arrows) or $CD44^+/SM22\alpha^+$ cells (orange arrows) in association with the *vasa vasorum* (VV). Dotted line indicates the position of the external elastic lamina between the adventitia (Adv) and the media (Me).

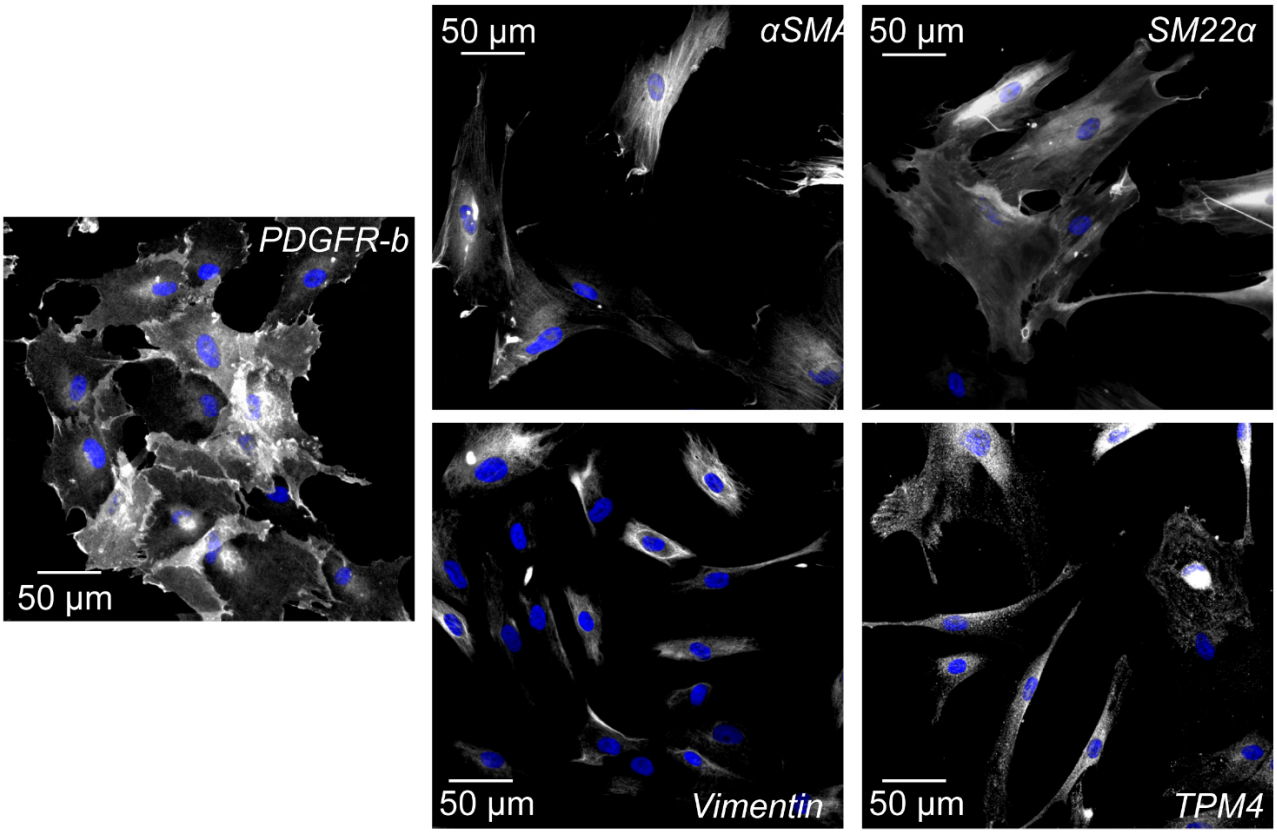

Figure S4. Characterization of SV-SMCs by immunofluorescence staining with anti PDGFR-b, αSMA, SM22α, Vimentin and Tropomyosin-4 (TPM4) specific antibodies.

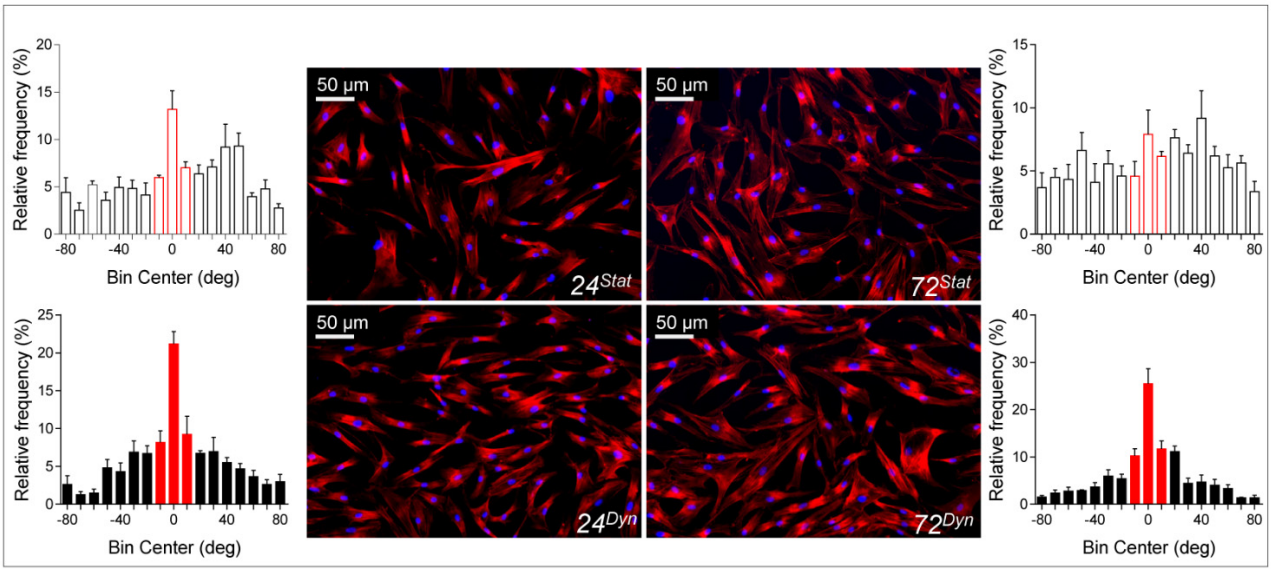

Figure S5. The panel shows the results of 24 and 72 h mechanical stimulation with a 10% uniaxial stretching regimen in the FlexCell device. The pictures in the centre show the structure of the F-actin cytoskeleton (in red, stained with Phalloidin-TRITC) in control and mechanically trained cells. The drawing in the upper part of the panel show the criterion that was adopted to assess the mechanical responses of the cells to cyclic elongation as already described by us. Namely, the frequency of the angles (θ) comprised between the major axis of the cell nuclei and an ideal orthogonal direction to the stretching were calculated and represented. From the graphical representation [23], it is evident that mechanically stimulated cells acquired a preferentially orthogonal specific orientation of their nuclei (red bars) demonstrating cytoskeleton rearrangements and mechano-sensitivity.

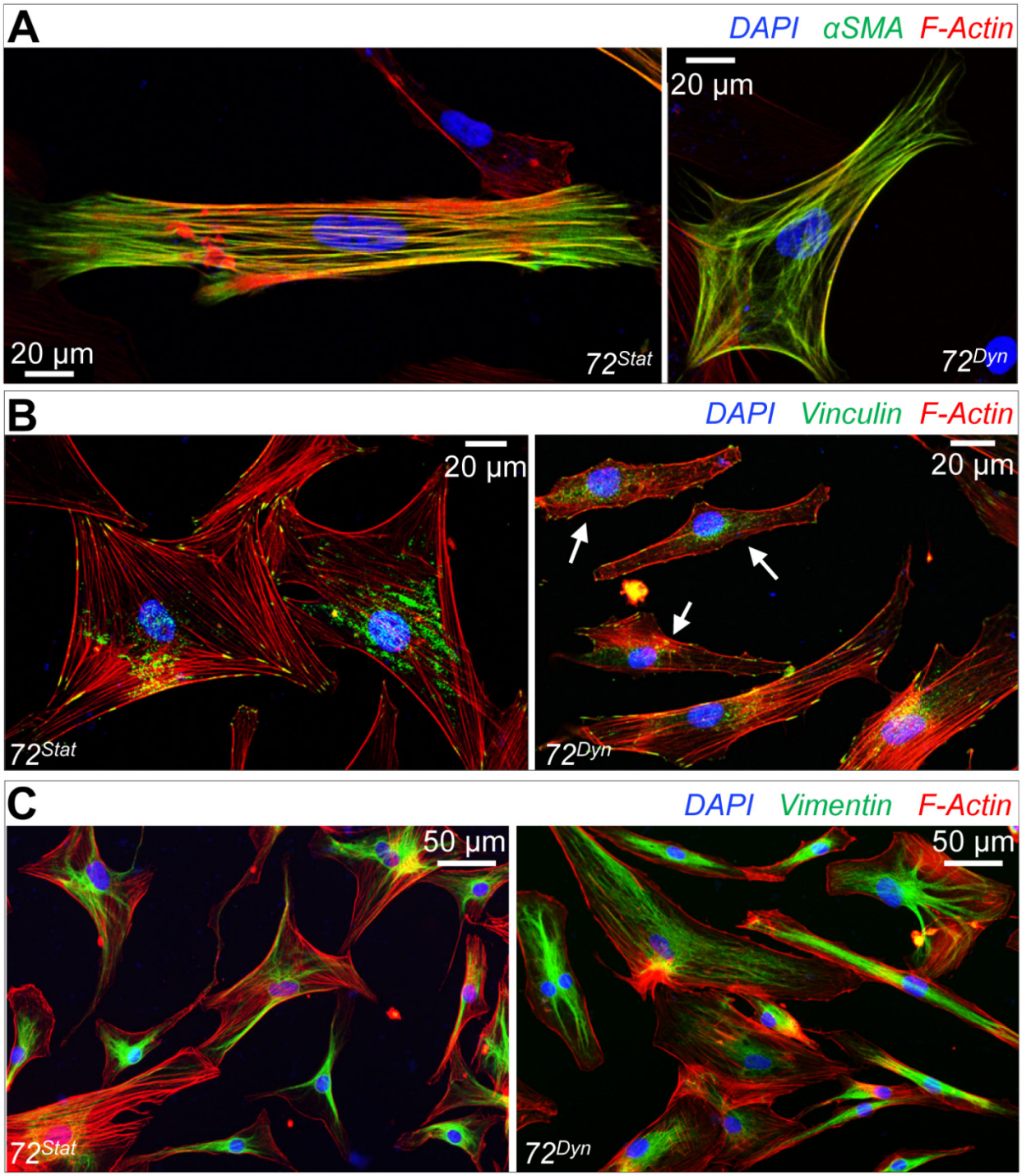

Figure S6. Immunofluorescence staining with antibodies for contractile/secretory phenotype in SV-derived SMCs subjected to mechanical strain for 72 h. In panel A, a double staining with Phalloidin-TRITC (red) and αSMA antibody (green) is shown in control cells and cells subjected to strain. Panel B represents the distribution of the focal adhesion contacts, as detected with Vinculin antibody (green dots connected to the F-actin cytoskeleton, red); arrows indicate cells with a lower organization of the F-Actin cytoskeleton and a reduced number of focal contacts. Panel C shows the expression and the intracellular distribution of Vimentin (green fluorescence). In keeping with previous data [24] and biochemical results shown in Figure 6B, the lower polymerization and organization of the αSMA^{+} fibres (A), the reduced number of focal contacts (B) and the higher presence of Vimentin (C), these staining confirm the phenotypical transition between the contractile (static) and the secretory (dynamic) phenotype of SV-SMCs.

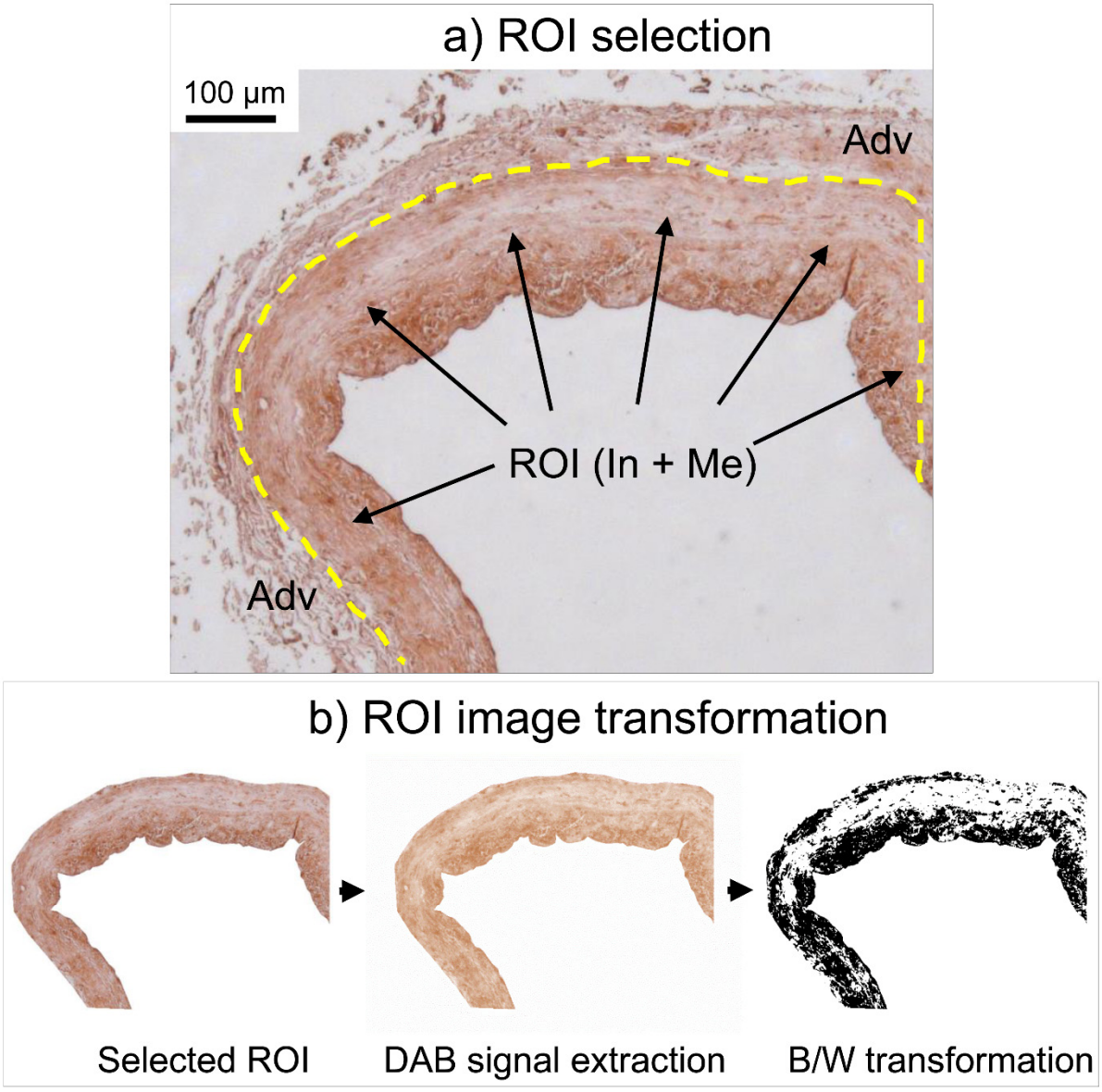

Figure S7. The upper picture shows the region of interest (ROI) in the vessel (comprising the media and the intima layers) where TSP-1 was quantified (see also **Figure 6D**). The lower panels show the Image J-based system used to quantify the expression of TSP-1 in the tissue. In order to make possible statistical comparisons (**Figure 6D**), the area (TSP-1^{+} area) occupied by black pixels was quantified and expressed as a percentage of the total area.

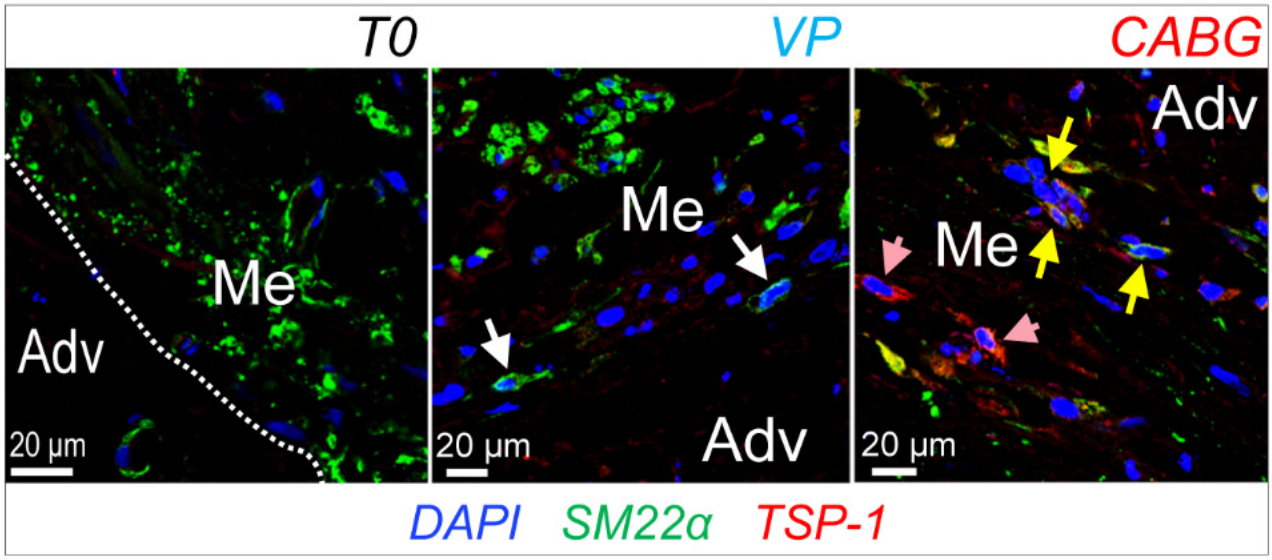

Figure S8. Immunofluorescence staining with antibodies recognizing SM22α (green fluorescence) and TSP-1 (red fluorescence) in SV samples before (T0) and after culture under venous (VP) or coronary (CABG) flow/pressure pattern for 14 days. It is evident that coronary flow mechanics increased expression of TSP-1 in cells expressing (yellow arrows) or not expressing (rose arrows) SM22α in the SV media. White arrows indicate $SM22\alpha^{+}$ in the picture showing the media of VP-treated SV sample.

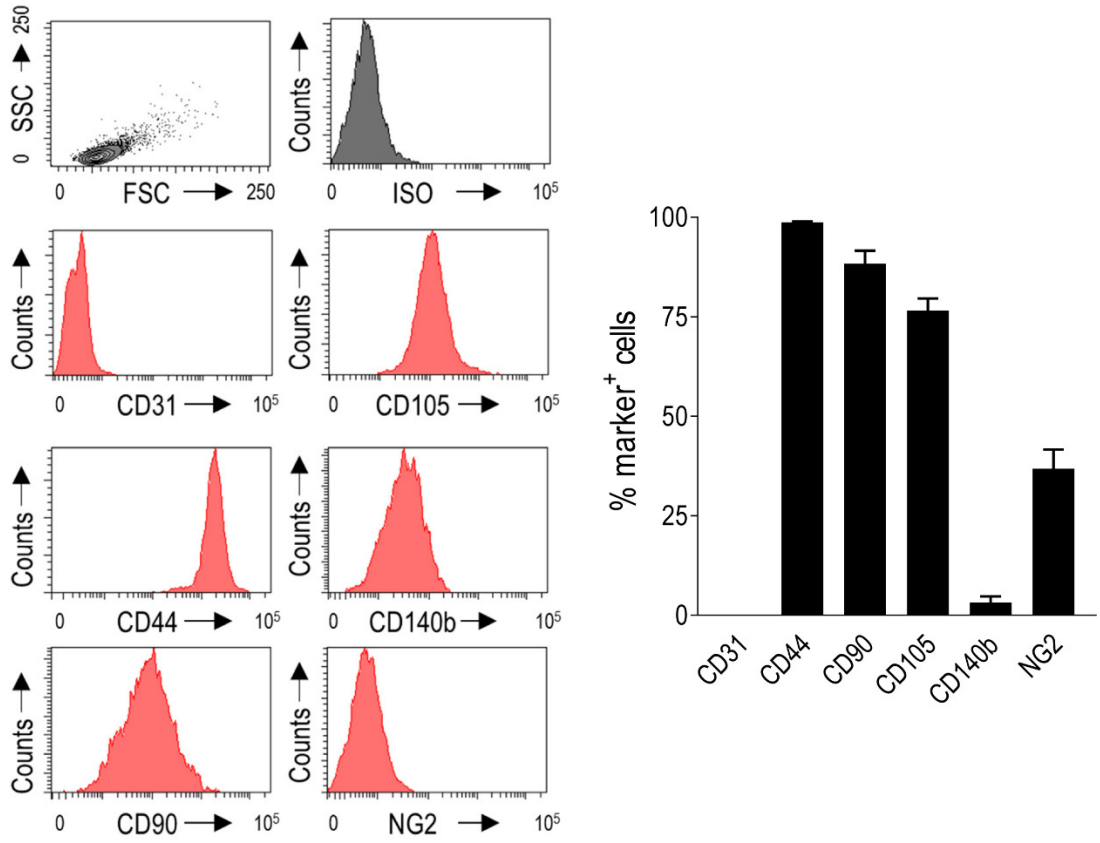

Figure S9. Characterization of human SVPs. Cells were culture amplified as described in methodological section and in reference publications[9, 25], exploiting their $CD34^{+}/CD31^{-}$ antigenic repertoire. As shown in the FACS histogram plots, SVPs expanded in culture expressed high levels of mesenchymal markers CD90, CD105 and CD44. NG2, a pericyte marker characterising cells in the SV *vasa vasorum* was, at least in part, downregulated. Bar graph represents average expression level and the relative SE of each marker in n = 37 SVPs preparations.

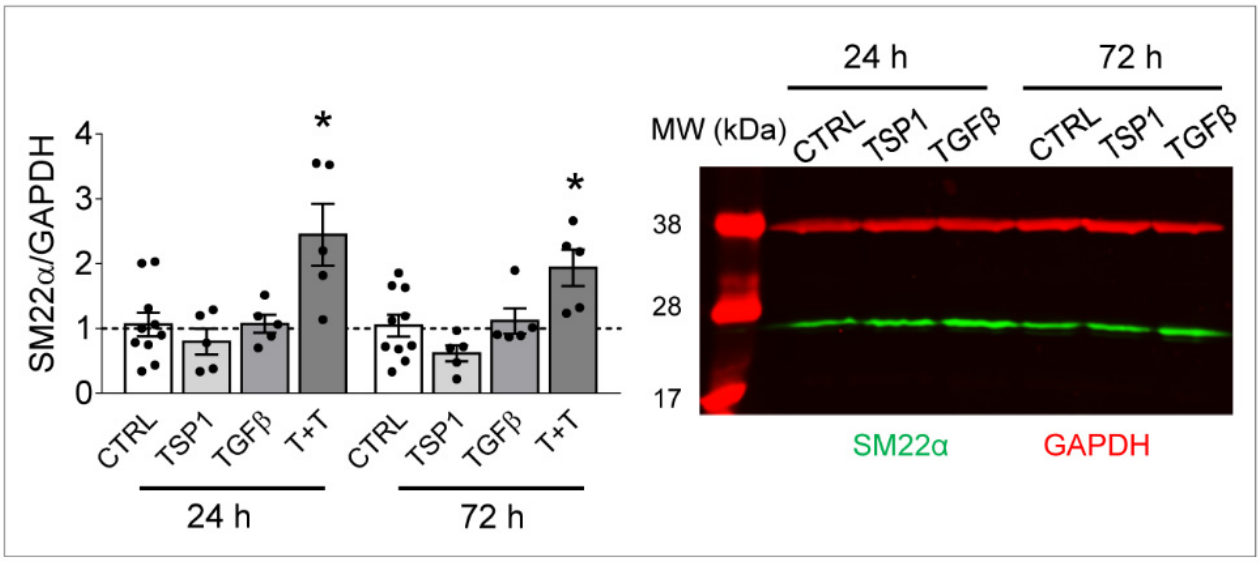

Figure S10. Effect of TSP-1 and TGF-β treatment on variations of SM22α expression in SVPs exposed to single or combined treatment (See also **Figure 7E**). * indicate $P < 0.05$ by one-way ANOVA with Newman-Keuls's comparison test. Bar graph represents mean and SE.

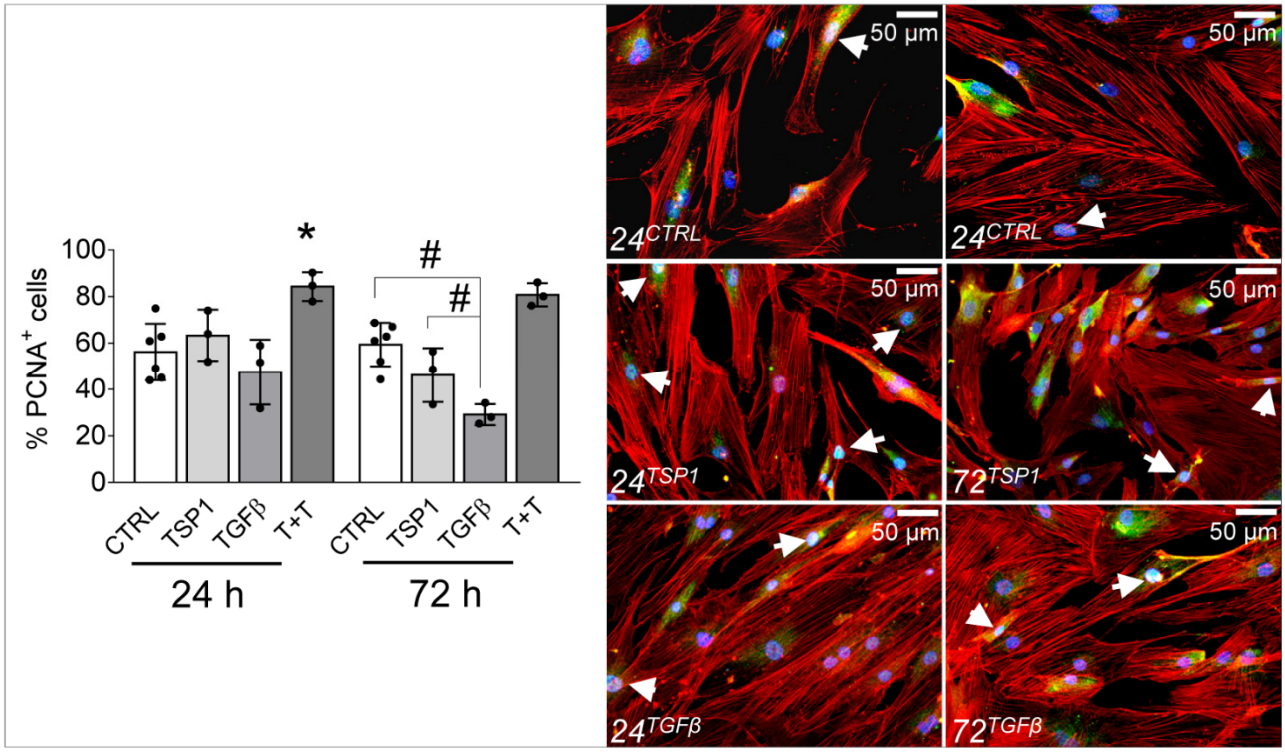

Figure S11. Effect of single/combined TSP-1/TGF-β treatment on variations in SVPs proliferation (**Figure 7F**). * indicate a statistically significant difference ($P < 0.05$) in the percentage of the $PCNA^+$ cells in cells treated with TSP-1 + TGF-β *vs.* all the other treatments at both time points. # indicate a statistically significant difference ($P < 0.05$) in the percentage of the $PCNA^+$ cells in TGF-β treatment *vs.* CTRL and TSP-1 treatment. Statistical analysis was performed by one-way ANOVA with Newman-Keuls multiple comparison post-*hoc* test. Bar graphs represent mean and SE of observations.

Variable	Saphenectomy patients (n = 66)	CABG patients (n = 21)
Age (y)	56 ± 13	68 ± 2
Male, n (%)	35 (53%)	19 (90%)
Hypertension, n (%)	16 (24.2%)	17 (94.4%)
Dyslipidaemia, n (%)	8 (12.1%)	10 (62.5%)
Diabetes, n (%)	3 (4.5%)	6 (35.3%)
Body mass index	26.5 ± 4.3	26.9 ± 0.6
Smoking, n (%)	22 (33.3%)	9 (42.9%)
Glycaemia	102 ± 25	
Creatinine	0.82 ± 0.2	

Table S1. Characteristics of the donors of cells (saphenectomy) and tissues (CABG surgery) collected for the study. Data are presented as percentages or mean ± SD.

24h stimulation

Description	t-test	FC (ON/OFF)	Peptide count	Unique peptides	Confidence score
Thrombospondin-1	**0.039**	**1.31**	**5**	**5**	**26.4**
Cathepsin L1	0.062	0.89	1	1	6.3
Glia-derived nexin	0.076	0.66	4	4	23.8
Collagen alpha-3(VI)	0.077	0.85	8	7	37.5
Actin_ cytoplasmic 1	0.085	1.10	3	3	17.4
Histone H2B type 1-K	0.11	1.20	1	1	6.6
Pentraxin-related protein PTX3	0.12	1.25	2	2	12.6
72 kDa type IV collagenase	0.13	0.75	2	2	10.9
Tenascin-X	0.167	1.49	3	3	15.3
Metalloproteinase inhibitor 1	0.19	0.64	3	3	20.4
Collagen alpha-1(III) chain	0.23	0.90	6	6	30.5
Transforming growth factor-beta-induced protein ig-h3	0.26	0.83	3	3	18.2
Galectin-3-binding protein	0.28	0.94	1	1	5.6
SPARC OS=Homo sapiens	0.30	1.11	3	3	16.8
Collagen alpha-1(VI) chain	0.37	1.09	6	6	31.2
Fibronectin	0.42	0.95	53	52	432.4
Collagen alpha-1(I) chain	0.45	0.91	29	7	194.3
Collagen alpha-1(II) chain	0.52	0.95	6	2	26.9
Decorin	0.61	1.03	6	6	32.9
Vimentin	0.67	1.06	6	6	32.1
Collagen alpha-2(I) chain	0.74	0.95	32	13	212.2
Collagen alpha-2(VI) chain	0.93	1.02	1	1	4.9

72h stimulation

Description	t-test	FC (ON/OFF)	Peptide count	Unique peptides	Confidence score
Collagen alpha-1(VI) chain	**0.009**	**0.82**	**24**	**23**	**195.6**
Pigment epithelium-derived factor	**0.013**	**0.87**	**6**	**6**	**37.7**
Thrombospondin-1	**0.029**	**1.99**	**21**	**20**	**154.8**
SPARC	**0.030**	**1.20**	**6**	**6**	**48.7**
Fibronectin	**0.042**	**0.68**	**79**	**37**	**779.8**
Cartilage oligomeric matrix protein	**0.043**	**0.82**	**7**	**7**	**69.1**
Collagen alpha-3(VI) chain	0.05	0.71	22	20	122.3
Target of Nesh-SH3	0.079	0.70	5	5	34.3
Decorin	0.091	0.77	11	9	71.2
Fibrillin-1	0.095	0.86	4	4	24.8
Collagen alpha-1(III) chain	0.12	0.83	44	35	332.4
Collagen alpha-2(VI) chain	0.13	0.90	14	12	82.5
Collagen alpha-1(I) chain	0.15	1.14	75	11	621.6
72 kDa type IV collagenase	0.19	0.84	6	6	42.7
Transforming growth factor-beta-induced protein ig-h3	0.19	0.71	8	8	49.1
Complement C1s subcomponent	0.24	0.87	6	6	38.8
Metalloproteinase inhibitor 2	0.28	0.77	2	2	18.8
L-lactate dehydrogenase A chain	0.28	0.92	6	5	36.9
Biglycan	0.41	1.20	6	4	42.1
Vimentin	0.41	1.09	19	18	125.8
Lumican	0.44	0.91	9	9	75.0
Galectin-3-binding protein	0.44	0.87	6	5	39.4
Lactadherin	0.59	0.93	4	3	23.0
Metalloproteinase inhibitor 1	0.59	0.94	6	6	48.2
Glia-derived nexin	0.73	1.08	11	11	75.6
Clusterin	0.74	1.04	9	9	71.0
Pentraxin-related protein PTX3	0.75	1.04	9	9	64.2
Follistatin-related protein 1	0.79	1.02	5	5	28.3
Collagen alpha-2(I) chain	0.87	1.01	67	34	584.3
Collagen alpha-1(XII) chain	0.92	1.01	28	25	172.8
Insulin-like growth factor-binding protein 7	0.93	0.99	8	7	62.4
Tenascin-X	0.95	0.99	29	27	171.9

Tables S2. Results of mass spectrometry-based secretome analysis on SMCs stimulated mechanically for 24 (n = 3) and 72 (n = 6) h. In red and green colors, respectively, are indicated secreted proteins with a significantly ($P < 0.05$; paired t-test) increased or decreased secretion in conditioned medium. Note the presence of Thrombospondin-1 as the unique factor secreted in higher amounts in mechanically stimulated SMCs *vs.* Controls at both time points.

Antibody/ Reagent	Host	Manufacturer	Clone, product code	Concentration tissue/cells
αSMA	Mouse	Dako	1A4, M0851	142 ng/mL tissue, 700 ng/mL cells
Calponin	Mouse	Abcam	PC10, ab65827	500 ng/mL tissue
CD44	Rat	Abcam	IM7, ab119863	20 µg/mL tissue
SM22α	Rabbit	Abcam	Polyclonal, ab14106	1.4 µg/mL tissue, 8 µg/mL cells
PCNA	Mouse	Dako	PC10, M0879	1.64 µg/mL tissue, 3.27 µg/mL cells
TSP-1	Mouse	Invitrogen	A6.1, MA5-13398	2 µg/mL tissue
TPM4	Mouse	Bio-Rad	4A4-1D2, MCA5263Z	5 µg/mL
Vimentin	Rabbit	Cell signaling technology	D21H3, #5741	Diluted as indicated
PDGFRβ	Rabbit	Cell Signaling Technology	28E1, #3169	Diluted as indicated
Vinculin	Rabbit	Invitrogen	42H89L44	5 µg/mL
Phalloidin	-	Sigma Aldrich	P1951	32 µg/mL
DAPI	-	Dako	D1306	50 µg/mL
488 mouse	Donkey	Invitrogen	A11034	4 µg/mL
488 rabbit	Goat	Invitrogen	A11034	4 µg/mL
546 mouse	Donkey	Invitrogen	A10036	4 µg/mL
546 rat	Goat	Invitrogen	A11081	4 µg/mL
546 rabbit	Goat	Invitrogen	A11010	4 µg/mL

Table S3. Reagents, primary and secondary antibodies employed for tissue and cell IF analysis.

Antibody	Host	Manufacturer	Concentration
αSMA	Mouse	Dako	7 µg/mL
Vimentin	Rabbit	Cell signaling technology	Diluted as indicated
TSP-1	Mouse	Invitrogen	200 ng/mL
SM22α	Rabbit	Abcam	1 µg/mL
GAPDH	Mouse/Rabbit	Santa-Cruz	200 ng/mL
680 anti-mouse	Donkey	LI-COR	100 ng/mL
680 anti-rabbit	Donkey	LI-COR	100 ng/mL
800 anti-mouse	Donkey	LI-COR	100 ng/mL
800 anti-rabbit	Donkey	LI-COR	100 ng/mL

Table S4. List of primary and secondary antibodies used for Western Blot.

Gene	Sequence
hTSP-1	Forward: 5’-TGAGGAGGACACTGGTAGAG-3’ Reverse: 5’-GGGCCTCAATGACAATTTCC-3’
hTAGLN	Forward: 5’-ACAAACTCATCTTCCTCAAGCC-3’ Reverse: 5’-CTTCTCATTTTCCATTCCCTTCAC-3’
hCOL1A1	Forward: 5’-GGACACAGAGGTTTCAGTGG -3’ Reverse: 5’-CCAGTAGCACCATCATTTCC -3’
hTGFβ-R	Forward: 5’-GCCAGTCCTAAGTCTGCAAT-3’ Reverse: 5’-GGTCTTGCCCATCTTCACA-3’
hGAPDH	Forward: 5’-AATCCCATCACCATCTTCCAG-3’ Reverse: 5’-AAATGAGCCCCAGCCTTC-3’

Table S5. PCR oligo sequences of primers employed in Q-RT-PCR analysis

Supplementary references

1. Dashwood MR, Tsui JC. 'No-touch' saphenous vein harvesting improves graft performance in patients undergoing coronary artery bypass surgery: A journey from bedside to bench. Vascul Pharmacol. 2013; 58: 240-50.
2. Johansson BL, Souza DS, Bodin L, Filbey D, Loesch A, Geijer H, et al. Slower progression of atherosclerosis in vein grafts harvested with 'no touch' technique compared with conventional harvesting technique in coronary artery bypass grafting: an angiographic and intravascular ultrasound study. Eur J Cardiothorac Surg. 2010; 38: 414-9.
3. Piola M, Ruiter M, Vismara R, Mastrullo V, Agrifoglio M, Zanobini M, et al. Full Mimicking of Coronary Hemodynamics for Ex-Vivo Stimulation of Human Saphenous Veins. Ann Biomed Eng. 2017; 45: 884-97.
4. Piola M, Prandi F, Bono N, Soncini M, Penza E, Agrifoglio M, et al. A compact and automated ex vivo vessel culture system for the pulsatile pressure conditioning of human saphenous veins. J Tissue Eng Regen Med. 2013.
5. Prandi F, Piola M, Soncini M, Colussi C, D'Alessandra Y, Penza E, et al. Adventitial vessel growth and progenitor cells activation in an ex vivo culture system mimicking human saphenous vein wall strain after coronary artery bypass grafting. PLoS ONE. 2015; 10: e0117409.
6. Castronuovo JJ, Smith TJ, Price RM. Validation of an in vitro model of human saphenous vein hyperplasia. J Vasc Surg. 2002; 35: 152-7.
7. Osgood MJ, Hocking KM, Voskresensky IV, Li FD, Komalavilas P, Cheung-Flynn J, et al. Surgical vein graft preparation promotes cellular dysfunction, oxidative stress, and intimal hyperplasia in human saphenous vein. J Vasc Surg. 2014; 60: 202-11.
8. Kenagy RD, Kikuchi S, Evanko SP, Ruiter MS, Piola M, Longchamp A, et al. Versican is differentially regulated in the adventitial and medial layers of human vein grafts. PLoS ONE. 2018; 13: e0204045.
9. Campagnolo P, Cesselli D, Al Haj Zen A, Beltrami AP, Krankel N, Katare R, et al. Human adult vena saphena contains perivascular progenitor cells endowed with clonogenic and proangiogenic potential. Circulation. 2010; 121: 1735-45.
10. Nikolaev NI, Müller T, Williams DJ, Liu Y. Changes in the stiffness of human mesenchymal stem cells with the progress of cell death as measured by atomic force microscopy. J Biomech. 2014; 47: 625-30.
11. Roeder BA, Kokini K, Sturgis JE, Robinson JP, Voytik-Harbin SL. Tensile Mechanical Properties of Three-Dimensional Type I Collagen Extracellular Matrices With Varied Microstructure. J Biomech Eng. 2002; 124: 214-22.
12. Goldstone RN, McCormack MC, Khan SI, Salinas HM, Meppelink A, Randolph MA, et al. Photochemical Tissue Passivation Reduces Vein Graft Intimal Hyperplasia in a Swine Model of Arteriovenous Bypass Grafting. J Am Heart Assoc. 2016; 5: e003856.
13. Szentiványi Jr M, Nádasy GL, Tóth M, Kopcsányi V, Jednákovits A, Monos E. Biomechanics of the saphenous artery and vein in spontaneous hypertension in rats. Pathophysiology. 1998; 4: 295-302.
14. Brioschi M, Lento S, Tremoli E, Banfi C. Proteomic analysis of endothelial cell secretome: A means of studying the pleiotropic effects of Hmg-CoA reductase inhibitors. J Proteomics. 2013; 78: 346-61.
15. Pontremoli M, Brioschi M, Baetta R, Ghilardi S, Banfi C. Identification of DKK-1 as a novel mediator of statin effects in human endothelial cells. Sci Rep. 2018; 8: 16671.
16. Brioschi M, Eligini S, Crisci M, Fiorelli S, Tremoli E, Colli S, et al. A mass spectrometry-based workflow for the proteomic analysis of in vitro cultured cell subsets isolated by means of laser capture microdissection. Anal Bioanal Chem. 2014; 406: 2817-25.

17. Roverso M, Brioschi M, Banfi C, Visentin S, Burlina S, Seraglia R, et al. A preliminary study on human placental tissue impaired by gestational diabetes: a comparison of gel-based versus gel-free proteomics approaches. Eur J Mass Spectrom (Chichester). 2016; 22: 71-82.
18. Angelini GD, Bryan AJ, Williams HM, Soyombo AA, Williams A, Tovey J, et al. Time-course of medial and intimal thickening in pig venous arterial grafts: relationship to endothelial injury and cholesterol accumulation. J Thorac Cardiovasc Surg. 1992; 103: 1093-103.
19. Thomas AC, Wyatt MJ, Newby AC. Reduction of early vein graft thrombosis by tissue plasminogen activator gene transfer. Thromb Haemost. 2009; 102: 145-52.
20. Vijayan V, Shukla N, Johnson JL, Gadsdon P, Angelini GD, Smith FCT, et al. Long-term reduction of medial and intimal thickening in porcine saphenous vein grafts with a polyglactin biodegradable external sheath. J Vasc Surg. 2004; 40: 1011-9.
21. Izzat MB, Mehta D, Bryan AJ, Reeves B, Newby AC, Angelini GD. Influence of external stent size on early medial and neointimal thickening in a pig model of saphenous vein bypass grafting. Circulation. 1996; 94: 1741-5.
22. McDonald RA, White KM, Wu J, Cooley BC, Robertson KE, Halliday CA, et al. miRNA-21 is dysregulated in response to vein grafting in multiple models and genetic ablation in mice attenuates neointima formation. Eur Heart J. 2013; 34: 1636-43.
23. Ugolini GS, Rasponi M, Pavesi A, Santoro R, Kamm R, Fiore GB, et al. On-chip assessment of human primary cardiac fibroblasts proliferative responses to uniaxial cyclic mechanical strain. Biotechnol Bioeng. 2016; 113: 859-69.
24. Worth NF, Rolfe BE, Song J, Campbell GR. Vascular smooth muscle cell phenotypic modulation in culture is associated with reorganisation of contractile and cytoskeletal proteins. Cell Motil Cytoskeleton. 2001; 49: 130-45.
25. Gubernator M, Slater SC, Spencer HL, Spiteri I, Sottoriva A, Riu F, et al. Epigenetic profile of human adventitial progenitor cells correlates with therapeutic outcomes in a mouse model of limb ischemia. Arterioscler Thromb Vasc Biol. 2015; 35: 675-88.